

THE INVERSE PROBLEM TO THE VORONOI DIAGRAM

A THESIS

SUBMITTED IN PARTIAL FULFILLMENT OF THE REQUIREMENTS

FOR THE DEGREE OF MASTER OF SCIENCE

IN THE GRADUATE SCHOOL OF THE

TEXAS WOMAN'S UNIVERSITY

COLLEGE OF ARTS AND SCIENCES

BY

LISA G. WINTER, B. S.

DENTON, TEXAS

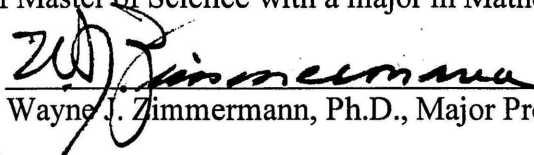
MAY 2007

TEXAS WOMAN'S UNIVERSITY  
DENTON, TEXAS

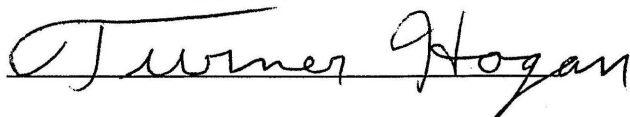
April 3, 2007

To the Dean of the Graduate School:

I am submitting herewith a thesis written by Lisa G. Winter entitled "The Inverse Problem to the Voronoi Diagram Problem." I have examined this thesis for form and content and recommend that it be accepted in partial fulfillment of the requirements for the degree of Master of Science with a major in Mathematics.

  
Wayne J. Zimmermann, Ph.D., Major Professor

We have read this thesis and recommend its acceptance:





  
Department Chair

Accepted:

  
Dean of the Graduate School



## ACKNOWLEDGEMENT

In pursuit of my masters degree I have had the support of many friends and my family. I would like to take the opportunity to thank each and every one of them. A very special thank you goes to my husband, Larry, who encouraged me to pursue the degree and carried through with a great deal of support. Last, but not least, I thank the professors who contributed their time and effort towards the completion of my degree; Dr. Zimmermann, Dr. Hamner, and Dr. Hogan. Specifically, I thank Dr. Zimmermann for his commitment and patience on assisting me with my thesis.

## ABSTRACT

LISA G. WINTER

### THE INVERSE PROBLEM TO THE VORONOI DIAGRAM

MAY 2007

The primary purpose of this thesis is to address the problem of solving the Inverse Problem for the Voronoi Diagram where the Inverse Problem is: Given a diagram that is in fact a Voronoi Diagram find the set of points  $X = \{x_1, x_2, x_3, \dots, x_n\}$  in  $R^2$  that will generate the diagram. In formulating a solution to the Inverse Problem it was necessary that we consider the problem of characterizing Voronoi Diagrams. In developing an algorithm for determining the generating set we considered questions of the form: Is the solution to the Inverse Problem unique? If the solution to the Inverse Problem is not unique, then what properties characterize the Voronoi Diagram? In addition we will develop solutions to a set of problems related to Voronoi Diagrams. These problems are related to: Given a finite set of points  $X = \{x_1, x_2, x_3, \dots, x_n\}$  in  $R^2$  find the domain of points  $N_k$  such that for every  $x \in N_k$ ,  $x_k$  is the nearest point to  $x$ , that is,  $\|x - x_k\| \leq \|x - x_j\|$  for every  $j \neq k$ .

## TABLE OF CONTENTS

ACKNOWLEDGEMENT .....	iii
ABSTRACT .....	iv
TABLE OF CONTENTS .....	v
LIST OF FIGURES .....	vii
Chapter	Page
I. PROBLEM STATEMENT.....	1
Introduction to Combinatorial Geometry .....	1
Statement of Problem .....	15
Outline of Thesis .....	16
II. REVIEW OF VORONOI DIAGRAMS IN $\mathbf{R}^2$ .....	18
Background.....	18
Voronoi Diagrams in $\mathbf{R}^2$ – Special Cases .....	27
Case 0 .....	27
Case 1 .....	28
Case 2 .....	30
The Points are Collinear .....	30
Non-Collinear .....	31
Voronoi Diagrams in Computer Science.....	33
Voronoi Diagrams in $\mathbf{R}^n$ .....	36
Voronoi Diagrams in $\mathbf{R}^2$ using the $L^\infty$ Norm .....	41
III. THE INVERSE VORONOI DIAGRAM PROBLEM .....	45
Ray Based Characteristics of Voronoi Diagrams in $\mathbf{R}^2$ .....	45
Inverse Voronoi Diagrams in $\mathbf{R}^2$ .....	55

Case 1. Zero Vertices.....	55
Case 2. One Vertex.....	58
Case 3. Two Vertices.....	63
Case 4. Three or More Vertices.....	64
IV. CONCLUSIONS AND OPEN PROBLEMS .....	65
Conclusions .....	65
Open Problems .....	66
BIBLIOGRAPHY .....	68

## LIST OF FIGURES

Figure 1.1. Partitioning of the Euclidean Plane, $R^2$ , using the nearpoint property relative to the given three stations. ....	2
Figure 1.2. A graphical representation in the plane of a linear program. ....	7
Figure 1.3. An illustration of the Stone-Tukey theorem in $R^2$ . ....	8
Figure 1.4. Again the Stone-Tukey applies, but finding the bisector in measure is even more difficult. ....	9
Figure 1.5. Plot of $X$ and its limit point $x^* = (1, 1)$ . ....	12
Figure 1.6. The line $L_1$ that contains those points having $x_1$ and $x_2$ as their nearpoints and the line $L_2$ that contains those points having $x_2$ and $x_3$ as their near points. ....	13
Figure 1.7. A Voronoi Diagram defines the structure of a Dragonfly's wing. ....	14
Figure 1.8. The veins of a peanut hull. ....	14
Figure 2.1. The grey area is defined by $R_{C(x),x_1} \cup R_{C(q),x_1}$ . ....	20
Figure 2.2. Plot of the Voronoi Diagram associated with the point set $X = \{X_1, \dots, X_6\}$ ....	21
Figure 2.3. The plot of the Delaunay triangulation associated with the Voronoi Diagram given in Figure 2.2. ....	21
Figure 2.4. Illustration of the proof of Theorem 2.3. ....	24
Figure 2.5. A plot of the average number of edges per polygon in a Voronoi Diagram versus $n$ . ....	27
Figure 2.6. Plot of the Voronoi Regions defined by the points $(0, 0)$ and $(1, 1)$ . ....	30
Figure 2.7. Plot of the Voronoi Regions defined by three collinear points. ....	30
Figure 2.8. Three noncollinear generating points of a Voronoi Diagram. ....	31

Figure 2.9. Sorting $X$ via the abscissa of each point $P_i$ can be done in linear time ..	35
Figure 2.10. The vertices of the tetrahedron define the generator set of the Voronoi Diagram which is defined by the ‘green’ planes.....	36
Figure 2.11. The shaded area, both light and dark, is the nearpoint area for $(-2,0)$ . Clearly it is nonconvex. ....	42
Figure 2.12. Note that the point $\mathbf{X}$ is not in the shaded area.....	43
Figure 2.13. Convexity is not present for either point.....	43
Figure 3.1. Diagram A is a 3-region Voronoi Diagram and Diagram B is a partition of the plane that is not a Voronoi Diagram for any three non-collinear points in the plane.....	46
Figure 3.2. Three point Voronoi Diagram [solid] generated by the set $\{(-3,0),(3,0),(0,3)\}$ .....	47
Figure 3.3. The Voronoi Diagram for the above four point case example has a unique generating point associated with the finite region .....	49
Figure 3.4. A geometric illustration of the argument given in the proof of Theorem 3.1 .....	51
Figure 3.5. The original Voronoi Diagram.....	53
Figure 3.6. Using $V_1$ we define the Voronoi Diagram $\mathcal{V}_1$ .....	54
Figure 3.7. Using $V_2$ we define the Voronoi Diagram $\mathcal{V}_1$ .....	54
Figure 3.8. Aligning the two Voronoi Diagrams $\mathcal{V}_1$ and $\mathcal{V}_2$ we have the resulting diagram with the two intersecting lines.....	54
Figure 3.9. The initial Voronoi Diagram with the $\beta$ ’s indicating the intersection of the rays with the overlaid circle .....	59
Figure 3.10. The angle of each region is represented by $\theta_k$ , $k = 1, 2, 3$ ; moving in a counterclockwise direction .....	60

Figure 3.11. An initial guess  $X_1$  is made then reflected through each ray,  
generating the set  $\{X_1, X_2, X_3, X_4\}$  .....60

Figure 3.12. Using  $X_1'$  reflection is applied to generate the set  $\{X_1', X_2', X_3'\}$  which  
is a generator set for the Voronoi Diagram .....61

Figure 3.13. The relationship between the angles as they are reflected through  
each ray.....62

## CHAPTER I

### PROBLEM STATEMENT

#### Introduction to Combinatorial Geometry

Imagine the situation, you are driving an automobile and it is nearly out of gas, but you know the location of three gas stations. Assuming that traffic is not a problem and knowing that the accuracy of your fuel gauge is doubtful you fear that the amount of fuel remaining is very low thereby compelling you to seek the nearest station. Thus given the location for each of three stations and your location there is a nearest station. In Figure 1 for the given position of  $x$  this would be Station A. If your location at the time of decision were different the nearest station might still be Station A, but then again it might be one of the remaining stations. Hence, with regards to Station A there exists a region satisfying the condition that Station A is the nearest station for any point in that region. The same can be said for the remaining stations. If the three regions were plotted as a map the boundaries defined by each region defines what is referred to as a Voronoi Diagram. In this example the Voronoi Diagram is defined by the three rays radiating from the vertex. Clearly any point on a ray different from the vertex has two stations as its nearpoints<sup>1</sup>. The vertex has all three stations as it

---

<sup>1</sup> Definition. A point  $x$  in the set  $X$  is the *nearpoint* of  $p$  if and only if for any  $y$  in the set  $X$ , then  $\|x - p\| \leq \|y - p\|$ .



nearpoints and any point strictly in the interior of a region has a unique nearpoint.

In Figure 1.1 the nearpoint to  $x$  is Station A.

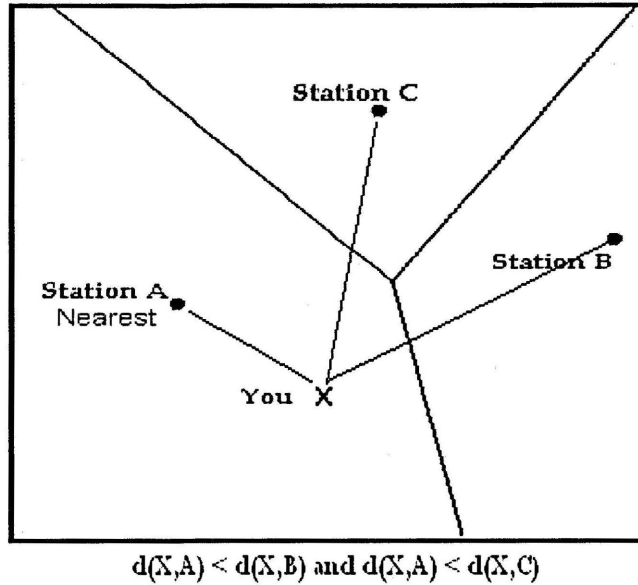


*Figure 1.1.* Partitioning of the Euclidean Plane,  $R^2$ , using the nearpoint property relative to the given three stations.

The mathematics of Voronoi Diagrams is an extensive subset of a much broader branch of mathematics known as combinatorial geometry. Included in this subject are concepts related to convexity<sup>2</sup>; which includes the well known Helly's Theorem, which states: Given  $n+1$  convex sets in  $R^n$  such that the intersection of any  $n$  sets is nonempty, then the intersection of all of the set is nonempty.

---

<sup>2</sup> Definition: A set  $A$  is said to be convex if and only if for any two points  $x, y \in A$  and any  $\theta$  in  $[0,1]$ ,  $\theta x + (1 - \theta)y \in A$ .

Combinatorial geometry also includes problems concerned with the approximation of a convex set by polygons, packing of a region with a fixed convex region, methods of cell decomposition using Dirichlet-Voronoi cells, the Minkowski-Hlawka Theorem, the Stone-Tukey Theorem, and Szemerédi-Borsuk's Problem to mention a few. In addition, there are numerous problems regarding nearpoint determination. With regards to these problems we should note that convexity plays an important role as is seen in Theorem 1.1. Convexity also plays an extensive role throughout the entire branch of mathematics known as combinatorial geometry as well as being a major subject in of itself. An excellent example of the use of convexity is given in the following theorem.

*Theorem 1.1.* Given a closed, convex set  $A$  in  $R^2$  and a point  $x$  not contained in  $A$  then there exists a unique nearpoint.

*Proof. Existence:* It suffices to note that  $A - x$ , which is the set of points defined by  $\{a - x : a \in A\}$ , is closed. Hence the set  $\{\|a - x\| : a \in A\}$  is bounded from below and is closed. Hence  $A - x$  has a greatest lower bound, thus for any  $a^* \in A$  such that  $\|a^* - x\| \leq \|a - x\|$  for all  $a \in A$ ,  $a^*$  is a nearpoint.

*Case 1:* Suppose  $A$  has nonempty interior, i.e., the measure of  $A$  is not zero. Let  $\alpha_1$  be any point in  $\text{int}(A)$ ,  $\alpha_1$  is not a nearpoint since for any circular neighborhood of  $\alpha_1$  there is a point nearer  $x$ .

*Case 2:* Suppose  $A$  has empty interior, i.e., the measure of  $A$  is zero. Let  $\alpha_1$  be any point in  $A$ . Since  $A$  is convex and has measure zero then  $A$  must be a line.

Hence  $\alpha_1$  is the nearpoint of  $x$  if and only if  $\alpha_1$  is the intersecting point of the line through  $x$  and perpendicular to  $A$ .

*Uniqueness:* Assume non-uniqueness, that is, there exist at least two nearpoints. Denote them by  $r$  and  $s$ , both in  $A$ . Now  $\|X - r\| = \|X - s\|$ . Further, the line segment joining  $X$  to  $r$  and  $X$  to  $s$  form two sides of an equilateral triangle. Since  $A$  is convex then the point  $(r + s) / 2$  is in  $A$ . Further the  $\|X - (r + s) / 2\| < \|X - r\|$ . Hence  $r$  cannot be a nearpoint.  $\square$

Although convexity plays a major role in geometry of Voronoi Diagrams, it is not limited in its application to the study. It should be noted that it also plays a major role in optimization theory, mathematical programming, and all flavors of geometry.

Applications of mathematical programming include linear programming, game theory and nonlinear programming with linear programming providing a method for modeling many activities related to scheduling. Of the scheduling problems there is the problem of scheduling airline flights and other transportation problems all being a special class of allocation problems. In fact there is a sizable segment of mathematics related to the Transportation Problem. It should be noted that the Transportation model is not restricted to problems of transportation since it is effectively an allocation problem. It has been used to optimize the production of men's pants for a major clothing manufacturer in the mid-1970s. Related to the Transportation Problem is an even weightier problem,

one that is closely coupled to the problem of *NP* (non-polynomial) completeness, namely the Traveling Salesman Problem. This problem has numerous applications some of which include robotic motion in the manufacturing of electronic boards.

Nonlinear programming is a mathematical program in which the objective function and/or the associated constraints are nonlinear. Such mathematical systems are used to model many applications. But finding the solution can be difficult hence they make use of numerical methods such as the gradient projection technique or Powell's Method for determining the solution. One class of nonlinear programs, namely the quadratic programming model, was used by the economist Harry Markowitz<sup>3</sup> to model the portfolio management problem which is now referred to as the Markowitz Portfolio Model. Finding the solution to this class of programs is straight forward by means of the Lagrangian method. It should be noted that the real problem in implementing this models is that of determining the parameters used to define the program.

With regards to linear programming the general form is given by

$$\begin{aligned}
 & \min \sum_{i=1}^n c_i x_i \\
 & \text{subject to:} \\
 & \sum_{i=1}^n a_{ij} x_i \leq b_j \quad j = 1, \dots, m \\
 & x_i \geq 0
 \end{aligned} \tag{1}$$

---

<sup>3</sup> Shared the 1990 Nobel Prize with Merton M. Miller and William F. Sharpe.

and the solution to this problem can be had, at least for small dimensional systems, by use of combinatorial geometry. From 1950 to approximately 1985 the standard method for solving a linear program is Dantzig's Simplex Method developed by Wood and Dantzig (1949), but this is beyond the scope of this thesis. Klee has shown that the Simplex Method is not the best method for some linear programs by demonstrating that for some cases it is not computational efficient. In the mid 1980s an alternate, more efficient method based on using the Interior Point Method was developed by Karmarkar (1984).

Since the optimal solution to a linear program will contain a vertex of the  $n$ -dimensional polygon described by the constraint set then, as indicated earlier, the linear program can be viewed as a problem in combinatorial geometry. Hence if the constraint set is defined by  $m$  inequalities then a combinatoric scheme would require that one solve  $\binom{m+n}{n}$ . This is almost always true since the set of inequalities generally requires that each variable be non-negative.

The geometric nature of a linear program is illustrated by use of the linear program given in equation (2).

$$\begin{aligned}
 &\max 4x_1 + 7x_2 \\
 &\text{subject to:} \\
 &2x_1 + x_2 \leq 4 \\
 &4x_1 + 6x_2 \leq 12 \\
 &x_1 \geq 0 \\
 &x_2 \geq 0
 \end{aligned} \tag{2}$$

where the shaded region in Figure 1.2 is the graphical representation of the problem's constraint set. In addition, the figure indicates three possible objective functions. The max-solution is a line parallel to the line  $4x_1 + 7x_2 = 0$  and containing the intersection point of the two lines defining the upper part of the feasible region.

It is well known that optimal solutions to any linear program contain at least one vertex of the constraint set, the polygon.

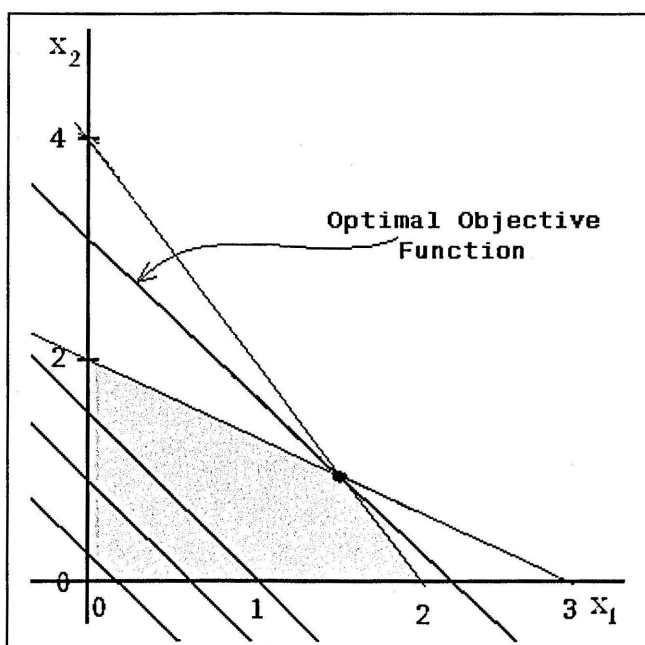


*Figure 1.2.* A graphical representation in the plane of a linear program as given by equation (2). The feasible region is shaded.

Another significant problem is the Stone-Tukey theorem, frequently referred to as the Ham Sandwich Theorem because of the analogy used to illustrate the

theorem, namely the ham sandwich. The theorem guarantees the existence of a hyperplane that bisects in measure  $n$  disjoint sets, see Figure 1.3. The theorem does not provide a method for finding the solution. Clearly the theorem does not provide uniqueness since there are many situations in which the solution is not unique as would be the case with two concentric circular regions.

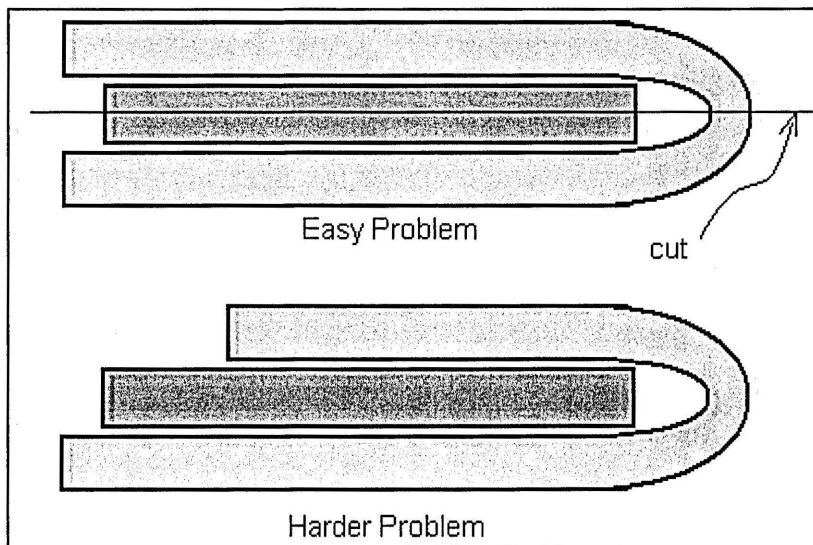


*Figure 1.3.* An illustration of the Stone-Tukey theorem in  $\mathbb{R}^2$ . The light grey set is horseshoed around the dark grey set. Finding the hyperplane that cuts the two sets in half is easily done in the Easy Problem. Although it is more difficult to find the hyperplane in the Harder Problem the Stone-Tukey Theorem guarantees the existence of such a cut.

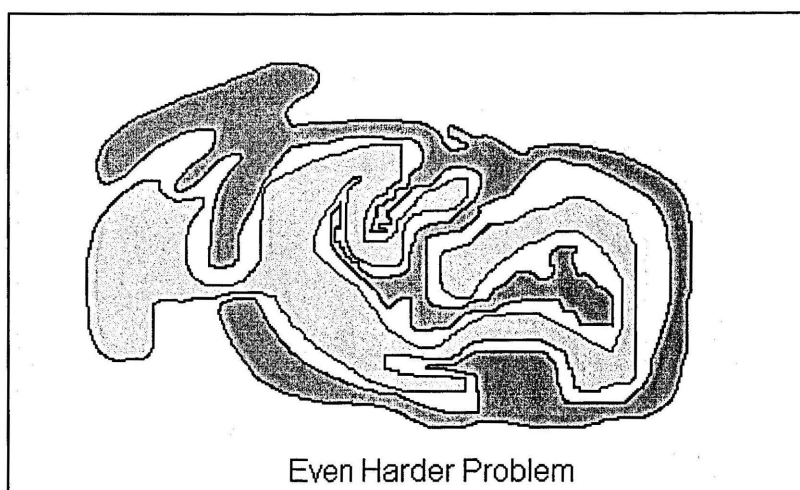


Figure 1.4. Again the Stone-Tukey applies, but finding the bisector in measure is even more difficult.

Beyer and Zardecki (2004) state that the earliest known paper *a propos* the Ham Sandwich Theorem, specifically for the case  $\mathbb{R}^3$ , was given by Steinhaus (1938). The theorem indicates that it is possible to bisect three solids with a plane. Steinhaus is credited with posing the problem while Stefan Banach is credited as being the first to solve the problem. He did this by reducing the theorem to the Borsuk-Ulam Theorem: Any continuous function from  $S^n$  to  $E^n$  maps some pair of antipodal points to the same point. Although it is referred to as the Ham Sandwich Theorem, initially it was informally posed in the following terms: “Can we place a piece of ham under a meat cutter so that meat, bone and fat are cut in halves?”

The theorem is given by:

*Theorem 1.2. (Stone–Tukey)* Given  $n$  regions with positive measure in  $\mathbb{R}^n$  there exists a single hyperplane that bisects each region.



We now consider the problem of finding near points, a much studied problem that plays a significant role in both mathematics and computer science. The simplest form of such a problem is the following:

Given  $n$  points  $\mathbf{X} = \{\mathbf{x}_1, \mathbf{x}_2, \mathbf{x}_3, \dots, \mathbf{x}_n\}$  in  $\mathbf{R}^n$  and a point  $\mathbf{x}^*$  find the point in  $\mathbf{X}$  nearest  $\mathbf{x}^*$ . Clearly, the simplest algorithm for finding the nearest point is  $O(n)^4$ .

The simplest algorithm would be:

1. Input the set of points  $\mathbf{X}$ .
2. Input  $\mathbf{x}^*$ .
3. Compute the distance  $d_1 = \|\mathbf{x}^* - \mathbf{x}_1\|$ .
4. Store the index, the point  $\mathbf{x}_1$ , and store the distance as  $d_s$ .
5. In a loop of length  $n - 1$ ,  $i = 2$  to  $n$ , perform the following:
  - a. Compute  $d_i = \|\mathbf{x}^* - \mathbf{x}_i\|$ .
  - b. If  $d_i < d_s$  then replace the stored values with the current index, current distance  $d_i$  and the current point,  $\mathbf{x}_i$ .

Clearly this algorithm will find the nearest point in  $n$  comparisons, hence, it is said to be  $O(n)^5$ .

---

<sup>4</sup>  $O(n)$  is a symbol used to measure the amount of work needed to complete a task. In this case the amount of work is linear in  $n$ . Thus, if the amount of data is doubled then the amount of work is doubled.

<sup>5</sup> Definition: Suppose  $f(x)$  and  $g(x)$  are two function defined on some subset of the reals, then  $f(x)$  is said to be  $O(g(x))$  as  $x$  approaches infinity if and only if there exists  $x_0$  and there exist  $M > 0$  such that  $|f(x)| \leq M |g(x)|$  for  $x > x_0$ .

This problem is much more difficult if the set  $X$  is not finite, but then the problem would not be in the realm of combinatorial geometry.

Example: If  $X = \{x : x = (1, 1 + (1/n)), n = 1, 2, 3, \dots\}$  and  $x^* = (1, 0)$  then there does not exist a nearpoint in  $X$  relative to  $x^*$ . Furthermore, the above algorithm would never cease execution. But using a limit concept one could find the greatest lower bound of 1 for the distance between  $x^*$  and  $x$ .

Further investigation leads to the following: For the given  $X$  any point in the half plane  $H = \{x : x = (x, y), y > 1\}$  has at least one nearpoint and for every  $x$  not in  $H$  there is no nearest point, but there is a greatest lower bound for the distance metric and a limit point  $(1, 1)$ . This is easily seen in Figure 1.5 to be the value  $\|x - (1, 1)\|$ . Further, uniqueness might not exist depending upon the value of  $x$ .

A similar problem is that of finding, if it exists, the nearest point of  $X$  where  $X$  is a region in  $R^2$  and  $x^*$  is the fixed point. Clearly if  $x^* \in X$  then  $x^*$  is the nearest point, else we must apply some methodology to obtain the nearest point. In addition we can again question uniqueness and existence.

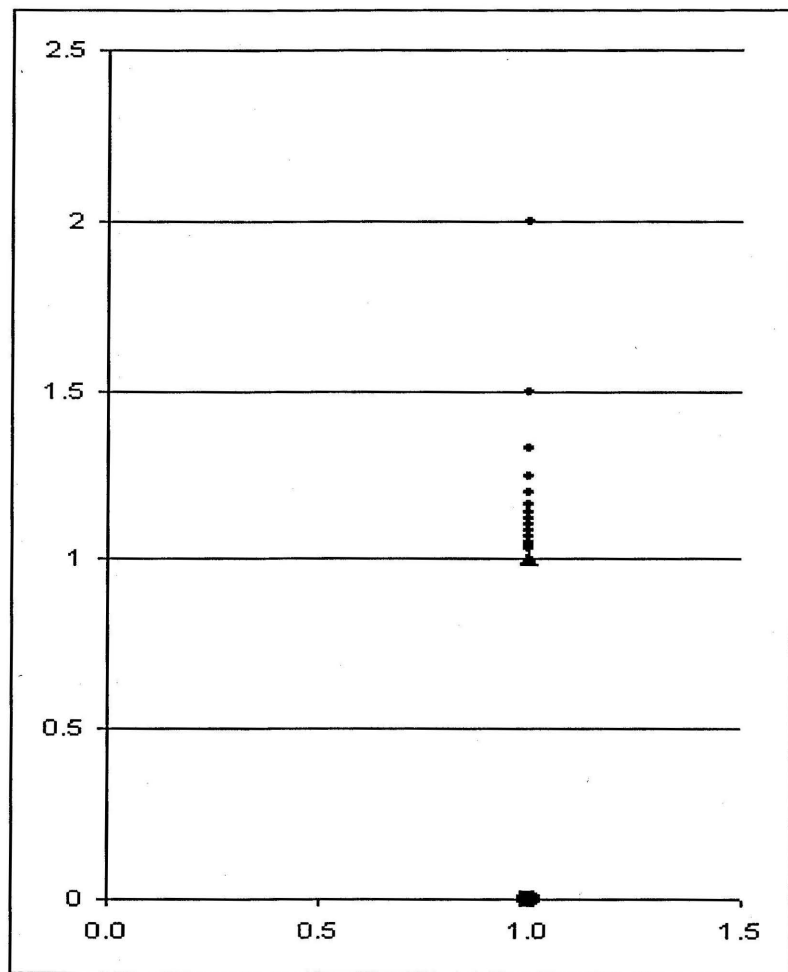


*Figure 1.5.* Plot of  $X$  and its limit point  $x^* = (1, 1)$ .

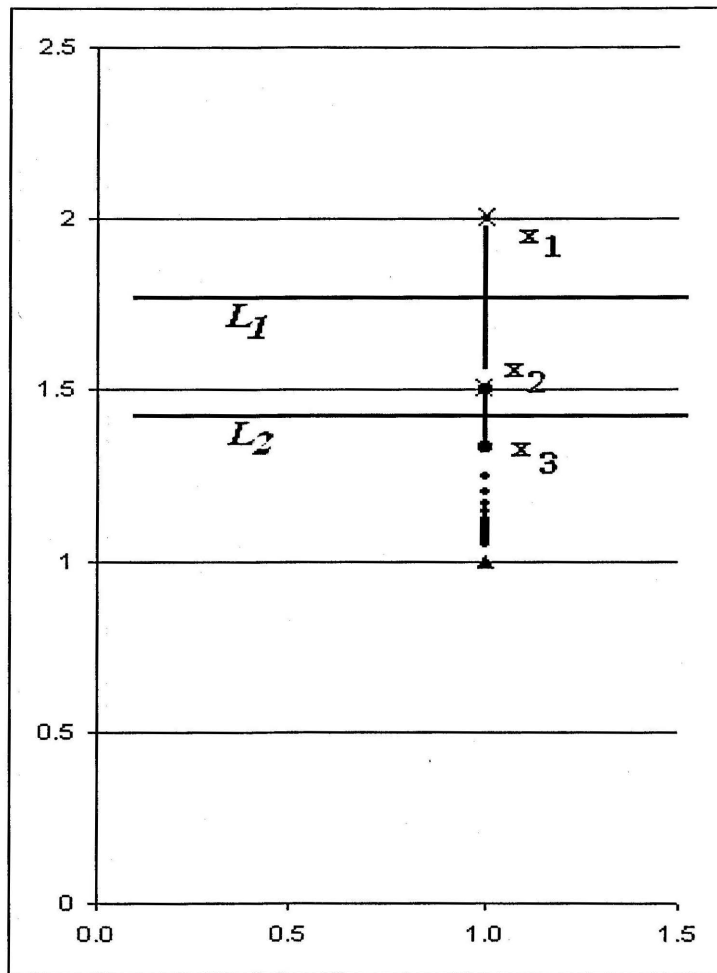


*Figure 1.6.* The line  $L_1$  that contains those points having  $x_1$  and  $x_2$  as their nearpoints and the line  $L_2$  that contains those points having  $x_2$  and  $x_3$  as their near points. In general the lines  $L_k$  for  $x_k$  and  $x_{k+1}$ .

Before closing our litany of related problems we should note, as indicated in Figure 1.7, that the structural foundation of a dragonfly's wing is defined by a Voronoi Diagram.

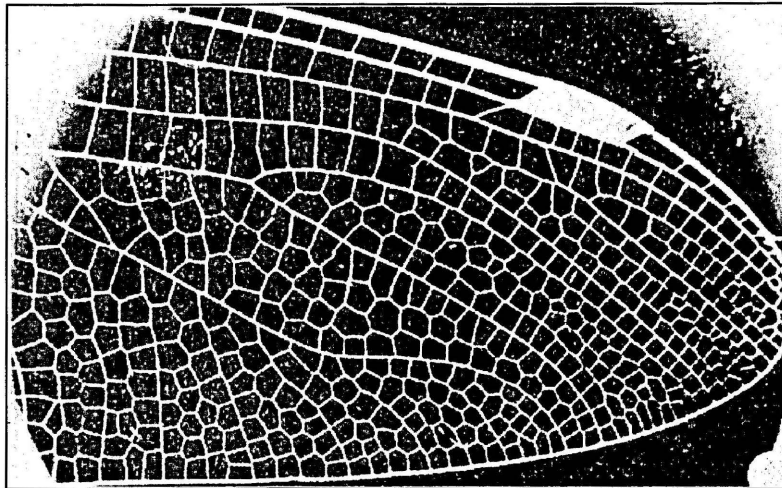


*Figure 1.7.* A Voronoi Diagram defines the structure of a Dragonfly's wing.

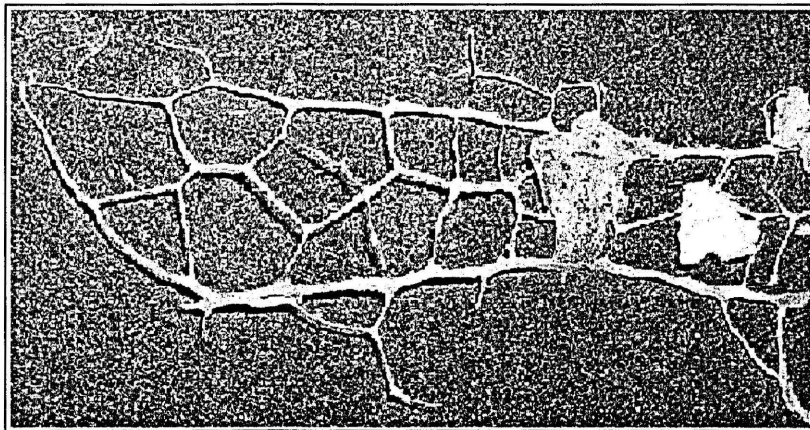


*Figure 1.8.* The veins of a peanut hull.

Although we do not know if the veins of a peanut hull define a Voronoi Diagram, but the following figure seems to imply such a geometric structure. With this we now consider the problems addressed by this thesis.

## Statement of Problem

In the previous section we have sought to find the nearpoint of a given point relative to a given set. A variation of this problem, the low-on-gas problem, is that of finding the collection of points nearest a specified point in a given, finite set of points. As indicated earlier the resulting diagram as defined by the boundaries of each region is called a Voronoi Diagram.

In solving the nearpoint problem as diagrammed in Figure 1.1 we considered a domain argument, that is, what domain, region  $V(x_i)$  in  $R^2$ , of points has the property that every point in  $V(x_i)$  has  $x_i$  as its nearpoint. We could extend this question to include: given the domain  $V(x_i)$  in  $R^2$ , find the sub-domain  $V''(x_i)$  such that every point in  $V''(x_i)$  has a unique nearpoint  $x_i$ . In our example every point on a line that is the perpendicular bisector of the line segment joining the two adjacent points in  $X$  does not have the property of uniqueness. See Figure 1.5. Hence  $V''(x_i)$  is the half plane above the line  $y = 1$  less the points in the line  $L_k$ .

Having considered the problem of finding a nearpoint and the domain of points having a particular nearpoint, unique or otherwise, we now consider the problems this thesis is to address.

Problem 1: Given a finite set of points  $X = \{x_1, x_2, x_3, \dots, x_n\}$  in  $R^2$  find the domain of points  $N_k$  such that for every  $x \in N_k$ ,  $x_k$  is the nearest point to  $x$ , that is,  $\|x - x_k\| \leq \|x - x_j\|$  for every  $j \neq k$ .

The solution to this problem results in a Voronoi Diagram, a topic that has been extensively studied in mathematics and computer science.

Problem 2: Have Voronoi Diagrams been characterized? If not, how can they be characterized?

Problem 3: Given a diagram that is in fact a Voronoi Diagram can we define the set of points  $X = \{x_1, x_2, x_3, \dots, x_n\}$  in  $\mathbf{R}^2$  that will generate the given diagram?

Problem 4: If there is a solution to Problem 3 is the solution unique?

Problem 5: If the solution to problem 4 is not unique what properties must the Voronoi Diagram possess?

Problem 6: How might the generating set for a Voronoi Diagram be determined?

### Outline of Thesis

Chapter 1 introduces the problems and ancillary material. Chapter 2 provides a survey of related material, namely, a review of basic concepts on Voronoi Diagrams. Chapter 2 will also provide a review of some results related to Voronoi Diagrams in  $\mathbf{R}^2$  with references to the extension of the work to  $\mathbf{R}^n$ . It should be noted that considerable work related to Voronoi Diagrams has been done in  $\mathbf{R}^2$ .

In addition numerous investigations of computer algorithms for generating Voronoi Diagrams can be found in O'Rourke [1998], DeBerg, van Kreveld,

Overmars & Schwarzkopf [2000], and Preparata & Shamos [1985]. Lastly we should point out that some work has been extended to the study of Voronoi Diagram in  $\mathbf{R}^n$ . Other directions include varied extensions of Voronoi Diagrams in  $\mathbf{R}^2$  and  $\mathbf{R}^3$  using weighted measure. This approach has some applications in biology, particularly in determining the size-distance and size-area relationships as measures of plant interactions. Given these remarks the work done in this thesis is restricted to  $\mathbf{R}^2$ . In particular we will address material related to Problems 1 and 2.

Chapter 3 addresses Problem 3, 4, 5 and 6. These problems are related to what we will refer to as the Inverse Voronoi Diagram Problem.

Chapter 4 provides a summary of the results followed by a set of open problems.



## CHAPTER II

### REVIEW OF VORONOI DIAGRAMS IN $\mathbf{R}^2$

#### Background

This chapter begin with a review of the salient features of Voronoi Diagrams as found in Okabe, Boots and Sugihara text, Spatial Tessellations: Concepts and Application of Voronoi Diagrams, and O'Rourke's text on Computational Geometry in C. Since these references provide proofs we will present only those which provide an insight to the methods used in proving various properties regarding Ordinary<sup>6</sup> Voronoi Diagrams. In addition, several concepts concerning nearpoints will be reviewed.

Note: For most of the thesis we will consider  $\|X\|$  to be the  $L_2$  norm on the plane  $\mathbf{R}^2$ .

Although defined in an earlier footnote, [1], we begin with the formal definitions of nearpoint.

*Definition 2.1.* Let  $X = \{X_1, \dots, X_n\}$  where  $n > 1$ . Let  $Y$  be a point in  $\mathbf{R}^2$  then the point  $X_1$  is said to be a nearpoint of  $Y$  if and only if  $\|Y - X_1\| \leq \|Y - X_j\|$  for all  $j > 1$ .

---

<sup>6</sup> The term Ordinary has been used since this chapter will provide an example of a Voronoi Diagram using a metric other than the  $L_2$  metric.

Although the following theorem will be stated and proved again it was felt that a geometric argument would provide significant insight to warrant Theorem 2.1 and the geometric proof.

*Theorem 2.1.* Let  $X = \{X_1, \dots, X_n\}$  where  $n > 1$  and let  $p$  and  $q$  be two point in  $\mathbb{R}^2$  such that  $X_1$  is a nearpoint of  $p$  and  $q$  then  $X_1$  is a nearpoint for any  $x \in [p, q]$ .

Proof. Let  $R_{C(p),X_1}$  denote the set of points in  $y \in \mathbb{R}^2$  such that  $\|y - p\| \leq \|p - X_1\|$ . Similarly  $R_{C(q),X_1}$  denotes the set of points in  $y \in \mathbb{R}^2$  such that  $\|y - q\| \leq \|q - X_1\|$ . Thus it follows that for every  $j > 1$ , the point  $X_j$  is not an element of  $R_{C(p),X_1} \cup R_{C(q),X_1}$ .

Now  $x \in [p, q]$  thus  $x = \theta p + (1 - \theta)q$  where  $0 \leq \theta \leq 1$ . Without loss of generality we will assume that  $x$  is in the region  $R_{C(q),X_1}$ . Further, suppose there is a point  $X_j$  in the generator set  $X$  such that  $X_j$  is the nearpoint of  $x$  then  $\|x - X_j\| \leq \|x - X_1\|$ . Thus  $X_j$  is in  $R_{C(x),X_1}$  which is in  $R_{C(p),X_1} \cup R_{C(q),X_1}$  by Figure 2.1. Thus

$X_j$  is in the set  $R_{C(p),X_1} \cup R_{C(q),X_1}$  which contradicts the fact that  $X_j$  is not in  $R_{C(p),X_1} \cup R_{C(q),X_1}$  for all  $j > 1$ .  $\square$

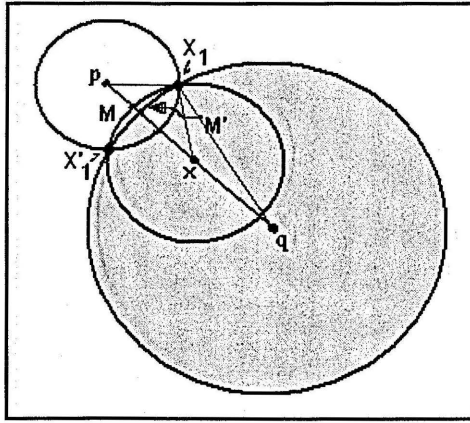


Figure 2.1. The grey area is defined by  $R_{C(x),X_1} \cup R_{C(q),X_1}$

*Definition 2.2.* Let  $X = \{X_1, \dots, X_n\}$  where  $n > 1$ , then the set of points in  $\mathbf{R}^2$  such that  $X_j$  is the nearpoint is denoted by  $V(X_j)$ , i.e.

$$V(X_j) = \{y \in \mathbf{R}^2 : \|y - x_i\| \leq \|y - x_j\| \forall j \neq i\}$$

*Definition 2.3.* Let  $X = \{X_1, \dots, X_n\}$  where  $n > 1$ , the set of points in  $\mathbf{R}^2$  such that  $X_j$  is the nearpoint region and is denoted by  $V(X_j)$ . The boundaries of  $V(X_j)$  for all  $j$  define the Voronoi Diagram and the set  $X$  is referred to as the generating points of the Voronoi Diagram.

Related to the concept of the Voronoi Diagram is the Delaunay triangulation.

*Definition 2.4.* The Delaunay triangulation is obtained from the Voronoi cells by connecting  $p, q$  in  $X$  by an edge if and only if the cells  $V(p)$  and  $V(q)$  are adjacent.

Below is an example of a Voronoi Diagram and its associate Delaunay triangulation is given in Figures 2.2 and 2.3 respectively.

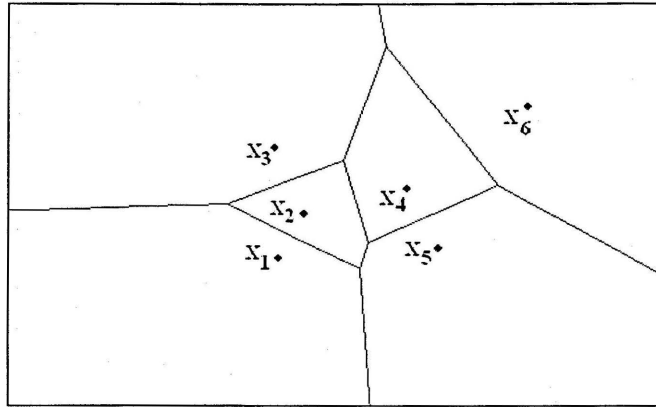


*Figure 2.2.* Plot of the Voronoi Diagram associated with the point set  $X = \{X_1, \dots, X_6\}$ . For any point in the region associated with  $X_i$  the point  $X_i$  is the nearpoint.

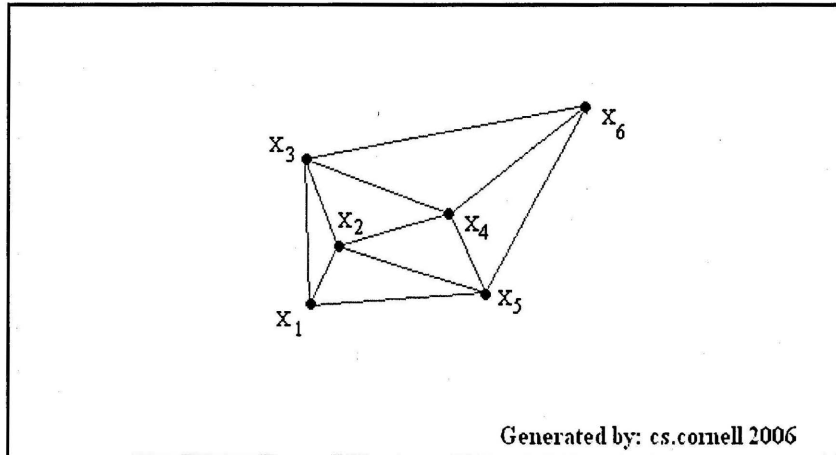


*Figure 2.3.* The plot of the Delaunay triangulation associated with the Voronoi Diagram given in Figure 2.2.

Although defined in the footnote [2] we formally define convexity.

*Definition 2.5.* A set  $X$  is said to be convex if and only if for any two points in the set the line segment joining the points is contained in  $X$ .

An equivalent statement requires that for any two points  $p$  and  $q$  in  $X$  and for every  $\theta \in [0, 1]$  the point  $\theta p + (1 - \theta) q \in X$ .

*Lemma 2.1.* Let  $A$  and  $B$  be convex sets then  $A \cap B$  is convex.

Proof. Let  $p$  and  $q$  be two points in  $A \cap B$ . Let  $x = \theta p + (1 - \theta) q$  where  $\theta$  is in the interval  $[0, 1]$ . Since  $A$  is convex  $x \in A$ . Similarly  $x \in B$ . Thus  $x \in A \cap B$ .  $\square$

*Lemma 2.2.* Let  $\{A_\alpha : \alpha \in \mathcal{A}, \mathcal{A} \text{ is a countable index set}\}$  then  $\bigcap_{\alpha} A_\alpha$  is convex.

Proof. Immediate by reason of Lemma 2.1.

*Lemma 2.3.* Let  $\mathcal{A}$  be a set of convex sets. The intersection of all the elements of  $\mathcal{A}$  is convex.

The set  $\mathcal{A}$  is not limited to countability.

The next theorem is a restatement of Theorem 2.1 in terms of convexity with a different proof, one that is based on the convexity of the intersection of half-planes.

*Theorem 2.2.* Let  $V(X_i)$  be the region generated by  $X_i$  of a Voronoi Diagram then  $V(X_i)$  is convex.

Proof: For each pair of points  $X_i$  and  $X_j$  in  $X$  the set of nearpoints to  $X_i$ , which we have denoted by  $V(X_i)$ , is contained in the closed half plane  $H(L(X_i, X_j), X_i)$  where the boundary of  $H(L(X_i, X_j), X_i)$  is a line perpendicular to the line segment

$LSeg(X_j, X_i)$  joining the point  $X_j$  and  $X_i$  and passing through the midpoint of the line segment. This must be true for any point  $X_j$ . Hence the set of points having  $X_i$  as its nearpoint is defined by  $\bigcap H(L(X_i, X_j), X_i)$ . Since each half plane is convex the set of points having  $X_i$  as its nearpoint is convex.  $\square$

**Theorem 2.3.**  $V(X_i)$  is unbounded if and only if  $X_i$  is an extremal point of the convex hull of  $X$ .

**Proof:** (Okabe, A., Boots, B., & Sugihara, K.) Under the non-collinearity assumption, assume that some generators are in the interior of  $CH(X)$ . We shall show that a Voronoi polygon whose generator is an interior point of  $CH(X)$  is finite. First, consider an interior generator point,  $p_i$  [ $p_i$  in Figure 2.4]. For  $X_i$  we can construct a triangle such that its vertices are generators on the boundary of  $CH(X)$ , say  $X_{i1}, X_{i2}, X_{i3} \in X$ , and it contains  $X_i$  in its interior [Figure 2.4]. We next construct the triangle by the intersection of the halfplanes  $H(X_i, X_{i1})$ ,  $H(X_i, X_{i2})$  and  $H(X_i, X_{i3})$  [the dashed lines in Figure 2.4]. Since  $X_i$  is an interior point of  $\Delta X_{i1}X_{i2}X_{i3}$ , this triangle is finite and

$$H(X_i, X_{i1}) \cap H(X_i, X_{i2}) \cap H(X_i, X_{i3}) \supset \bigcap_{j=1, j \neq i}^n H(X_i, X_j) = V(X_i).$$

The Voronoi polygon  $V(X_i)$  is thus finite.

Conversely, assume that the Voronoi polygon  $V(X_i)$  is bounded by Voronoi edges  $e(X_i, X_j)$ ,  $j \in J_i$ , where  $J_i$  is the set of indices of Voronoi polygons adjacent to  $V(X_i)$  (Figure 2.4). It is then obvious that  $X_i$  is in the interior of  $CH(\{X_j, j \in J_i\})$  (

the dashed lines in Figure 2.4). Since  $\text{CH}(\{X_j, j \in J_i\}) \subset \text{CH}(X)$ ,  $X_i$  is not on the boundary of  $\text{CH}(X)$ .

When generators are collinear, all generators are on  $\text{CH}(X)$  which degenerates into a line segment, and all Voronoi polygons are infinite.  $\square$

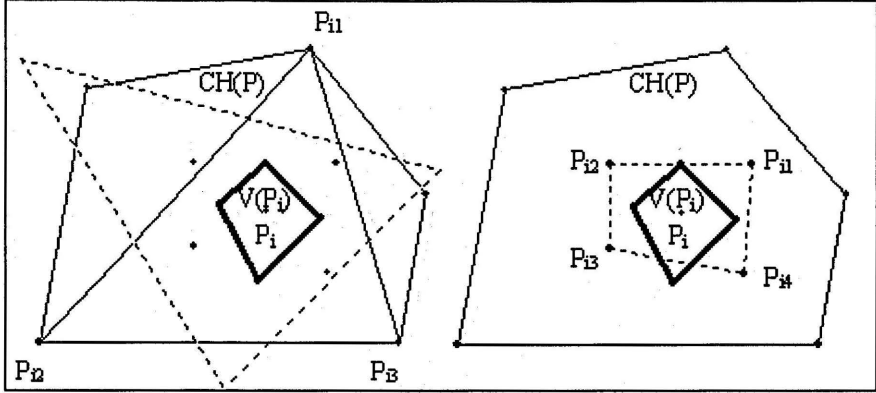


Figure 2.4. Illustration of the proof of Theorem 2.3.

**Definition 2.6.** A Voronoi Diagram is said to be degree  $n$  everywhere if and only if every vertex has  $n$  edges.

**Example.** The Voronoi Diagram given in the Figure 2.2 is of order 3 everywhere.

**Lemma 2.4.** Given  $n > 3$  let  $V$  be a Voronoi Diagram generated by the generator set  $\{X_1, X_2, \dots, X_n\}$ , then  $V$  is a Voronoi Diagram of degree  $n$  if and only if the points of the generator set are co-circular.

**Proof.** If the points of the generator set are co-circular then vertical bisections of any pair of points of the set must pass through the center of the circle defined by

$$C = \left\{ X : \|X - X_1\| = r, r = \|X_c - X_i\|, X_c = L_{B, X_1, X_2}^P \cap L_{B, X_1, X_3}^P \right\}$$

where  $L_{B,X_1,X_2}^P$  denotes the line that is the perpendicular bisector of the line segment joining  $X_1$  and  $X_j$ , where  $j > 1$  and  $X_c$  denotes the circle's center. Now  $X_1, X_2$ , and  $X_3$  defines the circle  $C_1$  and  $X_1, X_2$ , and  $X_4$  defines the circle  $C_2$ . Since the four points are on the same circle then  $C_1 = C_2$ , thus there is only one vertex for the Voronoi Diagram hence the vertex must be of degree four.

If the points are not co-circular, then  $X_1, X_2$ , and  $X_3$  define one circle  $C_1$  and the points  $X_1, X_2$ , and  $X_4$  define another one circle  $C_2$ . Since  $C_1 \neq C_2$  then the center of the circles  $C_1$  and  $C_2$  are distinct points. These two points define the vertices associated with the Voronoi Diagram and each is of degree three.  $\square$

*Theorem 2.4.* A Voronoi Diagram is degree three everywhere if and only if no four points are contained within a circle.

Proof. It suffices to note that proof is immediate by application of Lemma 2.3.

*Theorem 2.5.* For  $n \geq 3$ , the number of vertices in the Voronoi diagram of a set of  $n$  point sites in the plane is at most  $2n - 5$  and the number of edges is at most  $3n - 6$ .

Proof. If the sites are all collinear then there are  $n - 1$  parallel lines defining the Voronoi Diagram. Hence, the theorem follows immediately. If the points are not collinear we can make use of Euler's formula, which states that for any connected planar embedded graph with  $m_v$  nodes,  $m_e$  arcs, and  $m_f$  faces the following relation holds:

$$m_v - m_e + m_f = 2.$$



Attach an extra vertex,  $V_\infty$ , “at infinity” to the graph defined by the Voronoi Diagram by connecting all half-infinite edges to this vertex. We now have a connected planar graph to which we can apply Euler’s formula. We obtain the following relation between  $n_v$ , the number of vertices of the augmented graph,  $n_e$ , the number of edges and  $n$ , the number of regions:

$$(n_v + 1) - n_e + n = 2$$

$$n_v - n_e + n = 1$$

Moreover, every edge in the augmented graph has exactly two vertices, so if we sum the degrees of all vertices we get twice the number of edges. Because every vertex, including,  $V_\infty$ , has degree at least three we get

$$2n_e \geq 3(n_v + 1).$$

Hence the theorem follows.  $\square$

*Theorem 2.6.* The average number of edges per polygon in a Voronoi polygon is less than or equal to six.

*Proof.* Since every Voronoi edge is shared by exactly two Voronoi polygonal regions, then the average number of edges is given by  $2n_e/n$ . Since  $n_e \leq 3n - 6$  then the average number of Voronoi edges per ‘polygon’ is less than or equal to

$$(2(3n - 6))/n = (6 - 12/n) < 6. \quad \square$$

Figure 2.5 indicates the bounded growth of the average number of edges as  $n$  increases.

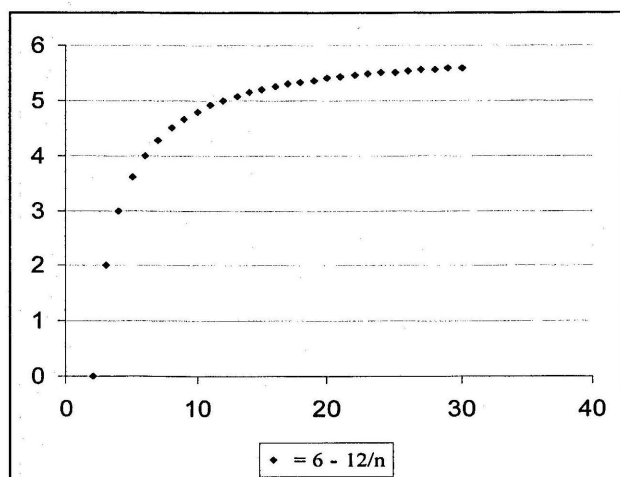


Figure 2.5. A plot of the average number of edges per polygon in a Voronoi Diagram versus  $n$ .

*Theorem 2.7.* The maximum number of bounded polygons in a Voronoi Diagram is  $n - 3$ .

*Proof.* It suffices to note that every generator set for a Voronoi Diagram must have at least three points in the convex hull of the generator set.  $\square$

### Voronoi Diagrams in $\mathbf{R}^2$ – Special Cases

Here we will look at the possible Voronoi Diagrams for various values of  $n$ ,  $n$  being the number of points in the generator set. Further we will assume that the norm of  $x \in \mathbf{R}^2$ ,  $\|x\|$ , is the  $L_2$  norm.

#### Case 0

For  $n = 1$  the Voronoi Diagram is null in that the entire plane is the region associated with the generator point.

### Case 1

For  $n = 2$  all situations are topologically equivalent, thus for this case there are two regions  $\mathcal{R}_1, \mathcal{R}_2$  such that the boundary of  $\mathcal{R}_1, \partial \mathcal{R}_1$ , is identical with the boundary for  $\mathcal{R}_2, \partial \mathcal{R}_2$ . Also,  $\text{Int}(\mathcal{R}_1) \cap \text{Int}(\mathcal{R}_2) = \emptyset$ . [Note.  $\text{Int}(S)$  denotes the interior of the set  $S$ , a subset of  $\mathbf{R}^2$ .]

In the following theorem we let  $\mathcal{P}$  be a finite set of points in  $\mathbf{R}^2$ , then

$$\mathcal{R}_k = \{ P \in \mathbf{R}^2 : \|P - P_k\| \leq \|P - P_i\|, i = 1, 2, \dots, n, P_i \in \mathcal{P} \}$$

*Theorem 2.8.* Let  $\mathcal{R}_i$  be the Voronoi region associated with  $P_i$  for  $i = 1, 2$ , then the boundary for  $\mathcal{R}_1, \mathcal{R}_2$  is the perpendicular bisector to the line segment  $\overline{P_1 P_2}$ .

*Proof:* Let  $P_1 = (x_1, y_1)$  and  $P_2 = (x_2, y_2)$  for  $\mathcal{R}_1$ , we have that  $\forall P \in \mathcal{R}_1$

$$\|P - P_1\| \leq \|P - P_2\|. \text{ Thus } \|(x, y) - (x_1, y_1)\|^2 \leq \|(x, y) - (x_2, y_2)\|^2 \text{ or}$$

$$\|(x - x_1, y - y_1)\|^2 \leq \|(x - x_2, y - y_2)\|^2.$$

Using the definition of the Euclidean Norm we have

$$(x - x_1)^2 + (y - y_1)^2 \leq (x - x_2)^2 + (y - y_2)^2$$

$$x^2 - 2xx_1 + x_1^2 + y^2 - 2yy_1 + y_1^2 \leq x^2 - 2xx_2 + x_2^2 + y^2 - 2yy_2 + y_2^2$$

$$-2xx_1 + x_1^2 - 2yy_1 + y_1^2 \leq -2xx_2 + x_2^2 - 2yy_2 + y_2^2$$

$$2xx_2 - 2xx_1 + 2yy_2 - 2yy_1 \leq x_2^2 - x_1^2 + y_2^2 - y_1^2$$

$$2(x_2 - x_1)x + 2(y_2 - y_1)y \leq (x_2 - x_1)(x_2 + x_1) + (y_2 - y_1)(y_2 + y_1)$$

$$(x_2 - x_1)x + (y_2 - y_1)y \leq (x_2 - x_1) \frac{(x_2 + x_1)}{2} + (y_2 - y_1) \frac{(y_2 + y_1)}{2}$$

Therefore we know that we have a bisector.

$$y \leq -\frac{(x_2 - x_1)}{(y_2 - y_1)}x + \left(\frac{x_2 - x_1}{y_2 - y_1}\right)\left(\frac{x_2 + x_1}{2}\right) + \left(\frac{y_2 + y_1}{2}\right)$$

The slope of the line through  $P_1, P_2$  is  $\frac{y_2 - y_1}{x_2 - x_1}$  while the slope of the line we just

derived is  $-\frac{x_2 - x_1}{y_2 - y_1}$ , the negative reciprocal. Since the point

$\left(\left(\frac{x_2 + x_1}{2}\right), \left(\frac{y_2 + y_1}{2}\right)\right)$  lies on the line given in (3.1) then the boundary is the

perpendicular bisector to the line segment  $\overline{P_1P_2}$ .  $\square$

Example:  $P_1 = (0, 0)$  and  $P_2 = (1, 1)$ . The equation for  $\mathcal{R}_1$  boundary line is

$$y \leq -\frac{(1-0)}{(1-0)}x + \left(\frac{1-0}{1-0}\right)\left(\frac{1+0}{2}\right) + \left(\frac{1+0}{2}\right)$$

$$y \leq -x + 1$$

where  $\mathcal{R}_1 = \{(x, y) \mid y \leq -x + 1\}$  and  $\mathcal{R}_2 = \{(x, y) \mid y \geq -x + 1\}$ . Figure 2.6

provides the Voronoi Diagram for the points  $(0,0)$  and  $(1, 1)$ .

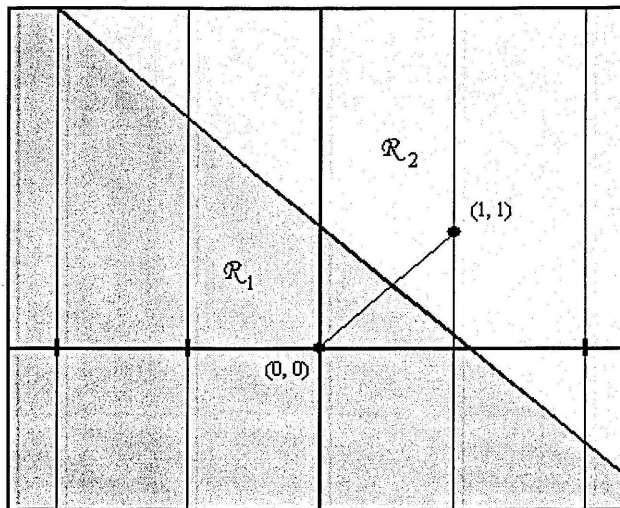


Figure 2.6. Plot of the Voronoi Regions defined by the points  $(0, 0)$  and  $(1, 1)$ .

### Case 2

For  $n = 3$  the points can either be collinear or non-collinear.

#### *The Points are Collinear.*

Here we can make use of the property presented in Case 1, namely that each boundary must be perpendicular to the same line  $L$  containing the three points.

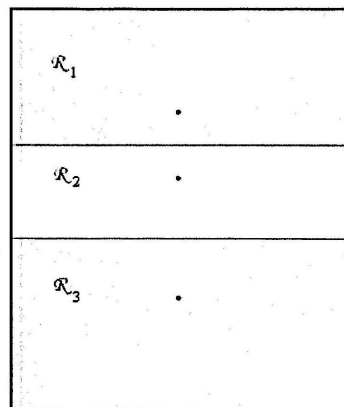


Figure 2.7. Plot of the Voronoi Regions defined by three collinear points.

We should note that  $\mathcal{R}_1$  is the intersection of two half planes, each containing  $P_1$ . Since the points are collinear the boundaries of the two half planes are parallel. Hence the region is defined by the boundary nearest the point since the associated half plane is contained strictly within the remaining half plane. A similar argument is made for the remaining regions,  $\mathcal{R}_2$  and  $\mathcal{R}_3$ .

### *Non-Collinear*

Here the three points define a triangle. Without loss of generality it is assumed that the three points are situated in such a manner that two of the points have the same abscissa, specifically zero. In this situation we obtain three regions,  $\mathcal{R}_1$ ,  $\mathcal{R}_2$ , and  $\mathcal{R}_3$ . The boundaries are defined by the three rays  $R_{1,2}$ ,  $R_{2,3}$ , and  $R_{1,3}$  which meet at the vertex  $V$ .

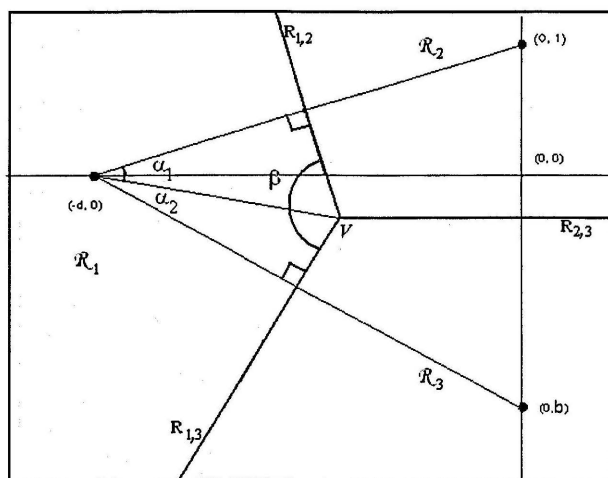


Figure 2.8. Three noncollinear generating points of a Voronoi Diagram. Thus the generating set is  $\{(0, 1), (0, b), (-d, 0)\}$

From Figure 2.8 we see that

$$\beta = \pi - \alpha_1 - \alpha_2$$

and since each of the triangles containing  $\alpha_1$  and  $\alpha_2$  are right triangles then

$0 < \alpha_1 < \frac{\pi}{2}$  and  $0 < \alpha_2 < \frac{\pi}{2}$ . Hence,  $0 < \alpha_1 + \alpha_2 < \pi$  which yields

$\pi > \pi - \alpha_1 - \alpha_2 > 0$ , thus  $\pi > \beta > 0$ . Hence,

$$\beta_1 + \beta_2 > \pi,$$

$$\beta_1 + \beta_3 > \pi,$$

and

$$\beta_3 + \beta_2 > \pi.$$

Hence, the following theorem.

*Theorem 2.9.* For any vertex of degree 3 in a Voronoi Diagram the sum of any two adjacent angles defined by the rays having that vertex as their origin is greater than  $\pi$ .

Note: If the Voronoi Diagram has a single vertex of degree four then it is possible that the sum of the angles of any two adjacent regions will sum to  $\pi$ . But, we can generalize Theorem 2.9 to the following:

*Theorem 2.10.* Given a Voronoi Diagram with a vertex of degree  $n$  then the sum of any  $n - 1$  adjacent angles defined by the rays is greater than  $\pi$ .

## Voronoi Diagrams in Computer Science

This section is concerned with the efficiency of an algorithm that generates a Voronoi Diagram and its dual, the Delaunay triangulation.

*Definition 2.7.* The Delaunay triangulation of a Voronoi Diagram is the graph obtained by connecting by an arc those points in the generating set  $X$  of the Voronoi Diagram having the property that their associated regions have a common boundary.

Much of the material in this section can be found in a paper on Voronoi Diagrams by Franz Aurenhammer and Rolf Klein. They discussed several ways of computing the Voronoi Diagram and its dual, the Delaunay tessellation. For simplicity, we assume that no four points of  $X$  are cocircular and that no three of them are collinear then the dual of the Voronoi diagram  $V(X)$  is a triangulation of  $X$ . Hence three points of  $X$  give rise to a Delaunay triangle if and only if their circumcircle does not contain a point of  $X$  in its interior. Thus all algorithms in their paper can be made to run without the general position assumption.

We first note that the data structures suited for working with planar graphs like the Voronoi diagram are the doubly connected edge list (DCEL) and the quad edge structure (QES). In either structure, a record is associated with each edge  $e$  that stores the following information: the names of the two endpoints of  $e$ ; references to the edges clockwise or counterclockwise next to  $e$  about its endpoints; finally, the



names of the faces to the left and to the right of  $e$ . The space requirement of both structures is  $O(n)$ .

Either structure allows efficient traversal of the edges adjacent to a given vertex, and the edges bounding a face. The quad edge structure offers the additional advantage of describing, at the same time, a planar graph and its dual, so that it can be used for constructing both the Voronoi diagram and the Delaunay triangulation.

From the DCEL of  $V(X)$  we can derive the set of triangles constituting the Delaunay triangulation in linear time,  $O(n)$ . However, how this is done is beyond the scope of this paper. Conversely, from the set of all Delaunay triangles the DCEL of the Voronoi diagram can be constructed in time,  $O(n)$ . Therefore, each algorithm for computing one of the two structures can be used for computing the other one, within  $O(n)$  extra time.

Aurenhammer and Klein indicated that it is convenient to store structures describing the finite Voronoi diagram in such a manner that the convex hull of the point sites can be easily reported by traversing the bounding curve. In doing this they made use of the fact that the average number of edges to a region is less than six.

Before constructing the Voronoi diagram they established a lower bound for the computational complexity.

Suppose that the  $n$  real numbers, denoted by  $x_1, \dots, x_n$  are given. From the Voronoi diagram of the point set  $X = \{P_i = (x_i, x_i^2) \mid 1 \leq i \leq n\}$  one can derive, in

linear time, the vertices of the convex hull of  $X$  in counterclockwise order. From the leftmost point in  $X$  on, this vertex sequence contains all points  $P_i$ , sorted by increasing values of  $x_i$ , see Figure 2.9.

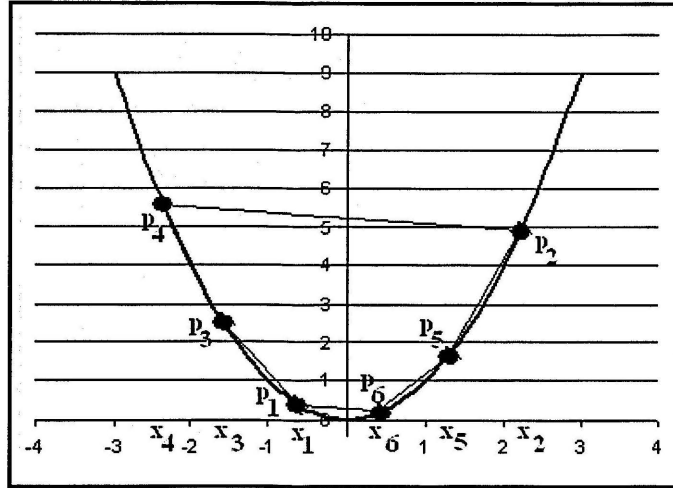


Figure 2.9. Sorting  $X$  via the abscissa of each point  $P_i$  can be done in linear time.

This argument due to Shamos shows that constructing the convex hull and, *a fortiori*, computing the Voronoi diagram, is at least as difficult as sorting  $n$  real numbers, which requires  $\Theta(n \log n)$  time in the algebraic computation tree model.

However, a point of argument is lost in this reduction. After sorting  $n$  points by their  $x$ -values, their convex hull can be computed in linear time, whereas sorting does not help in constructing the Voronoi diagram.

**Definition 2.8.** A function  $f$  is said to be asymptotically bounded by  $g$  if  $\exists M > 0, \exists x_0 : |f(x)| \geq M|g(x)| \forall x > x_0$ .

We denote this by  $f(n) \in \Omega(g(n))$ .

*Theorem 2.11.* It takes  $\Omega(n \log n)$  to construct the Voronoi diagram of  $n$  points  $\{P_1, \dots, P_n\}$  whose  $x$ -coordinates are strictly increasing.

The proof of this theorem can be found in Aurenhammer and Klein's notes and is omitted.

### Voronoi Diagrams in $\mathbf{R}^n$ .

Although the chapter's title is Voronoi Diagrams  $\mathbf{R}^2$  some of what we have developed can be extended to a higher dimensional space such as  $\mathbf{R}^3$ . In  $\mathbf{R}^3$  we would use the plane that passes through the midpoint of the line connecting two points from the generating set  $X$  and perpendicular to the line. This is readily seen in Figure 2.10.

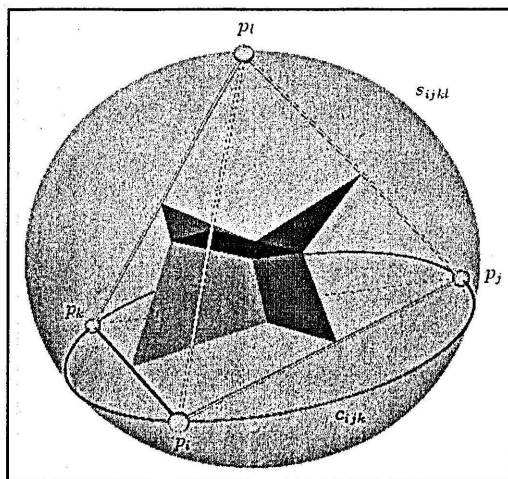


*Figure 2.10.* The vertices of the tetrahedron define the generator set of the Voronoi Diagram which is defined by the 'green' planes. Note that the region for each  $p_i$  is convex.

An immediate extension is that of convexity of each region of a Voronoi Diagram in  $\mathbf{R}^2$ . This property can be extended to  $\mathbf{R}^3$  and even to  $\mathbf{R}^n$  since each region is the intersection of convex half-spaces. Furthermore, in  $\mathbf{R}^2$  the vertices of the Voronoi Diagram are simply the intersection of two lines. Thus the finite regions consist of edges and vertices, whereas, in  $\mathbf{R}^3$  the finite regions consist of faces, edges and vertices. Clearly, Euler's theorem is applicable since the regions are polytopes.

Since our first theorem relates to the measure of an angle we recall that solid angles are measured in steradians. In  $\mathbf{R}^2$  an angle is measured in radians with  $2\pi$  being the period. Thus a point at (1,0) can slide along a circle of radius 1 and return to the initial position after traveling through a distance of  $2\pi$  units where  $2\pi$  is the circumference of the unit circle. Similarly, for  $\mathbf{R}^3$  a unit sphere is used and the 'angle' is measured in steradians with the 'complete' sweep being  $4\pi$ . Earlier we noted that if at a vertex of degree 3 of a Voronoi Diagram in  $\mathbf{R}^2$  we sum any two adjacent angles defined by the 'rays' extending from this vertex the sum is greater than  $\pi$ . Here we can extend this to the following conjecture.

*Conjecture 2.1.* Given a Voronoi Diagram in  $\mathbf{R}^3$  and a vertex of degree four, then the sum of the steradians of any two adjacent regions is greater than  $2\pi$ .

First we consider will the following Lemma.

*Lemma 2.5.* Any four non-coplanar points in  $\mathbf{R}^3$  are contained in a unique sphere.

Proof. Let  $x_1, x_2, x_3$ , and  $x_4$  be the four points. Let  $x_c$  denote the center of the sphere. This requires that  $\|x_1 - x_c\| = \|x_2 - x_c\| = \|x_3 - x_c\| = \|x_4 - x_c\|$  which yield the system

$$\|p_1 - p_c\| = \|p_2 - p_c\|$$

$$\|p_1 - p_c\| = \|p_3 - p_c\|$$

$$\|p_1 - p_c\| = \|p_4 - p_c\|$$

which is equivalent to the following:

$$p_1 \cdot (\overline{p_1} - 2\overline{p}) = p_2 \cdot (\overline{p_2} - 2\overline{p})$$

$$p_1 \cdot (\overline{p_1} - 2\overline{p}) = p_3 \cdot (\overline{p_3} - 2\overline{p})$$

$$p_1 \cdot (\overline{p_1} - 2\overline{p}) = p_4 \cdot (\overline{p_4} - 2\overline{p})$$

which is equivalent to the following three by three system.

$$\begin{bmatrix} x_2 - x_1 & y_2 - y_1 & z_2 - z_1 \\ x_3 - x_1 & y_3 - y_1 & z_3 - z_1 \\ x_4 - x_1 & y_4 - y_1 & z_4 - z_1 \end{bmatrix} \begin{bmatrix} x \\ y \\ z \end{bmatrix} = \begin{bmatrix} (p_2 \cdot p_2 - p_1 \cdot p_1)/2 \\ (p_3 \cdot p_3 - p_1 \cdot p_1)/2 \\ (p_4 \cdot p_4 - p_1 \cdot p_1)/2 \end{bmatrix}$$

Since the four points are non-coplanar the three by three matrix is nonsingular and has a unique solution.  $\square$

Hence we can now prove the following theorem.

*Theorem 2.12.* Given a Voronoi Diagram,  $\mathcal{V}$ , in  $\mathbb{R}^3$  generated by four non-coplanar points then the six perpendicular bisecting planes of  $\mathcal{V}$  must intersect at a single point.

Proof. Since the four points are non-coplanar the resulting convex hull is a tetrahedron with six edges, four faces, and each face being a triangle. Further, for each of the six perpendicular bisectors we have the following:

$$\|p_1 - p_c\| = \|p_2 - p_c\| = \|p_3 - p_c\| = \|p_4 - p_c\|$$

which yields four systems. Let  $S_1$  be the first system, namely,

$$\|p_1 - p_c\| = \|p_2 - p_c\|$$

$$\|p_1 - p_c\| = \|p_3 - p_c\|$$

$$\|p_1 - p_c\| = \|p_4 - p_c\|.$$

In this  $p_1$  is contained in every equation. This system can be written as

$$-2\overline{p} \cdot \overline{p_1} + \overline{p_1} \cdot \overline{p_1} = -2\overline{p} \cdot \overline{p_2} + \overline{p_2} \cdot \overline{p_2}$$

$$-2\overline{p} \cdot \overline{p_1} + \overline{p_1} \cdot \overline{p_1} = -2\overline{p} \cdot \overline{p_3} + \overline{p_3} \cdot \overline{p_3}$$

$$-2\overline{p} \cdot \overline{p_1} + \overline{p_1} \cdot \overline{p_1} = -2\overline{p} \cdot \overline{p_4} + \overline{p_4} \cdot \overline{p_4}.$$

Reorganizing the terms we have

$$2(\overline{p_2} - \overline{p_1}) \cdot \overline{p} = \overline{p_2} \cdot \overline{p_2} - \overline{p_1} \cdot \overline{p_1}$$

$$2(\overline{p_3} - \overline{p_1}) \cdot \overline{p} = \overline{p_3} \cdot \overline{p_3} - \overline{p_1} \cdot \overline{p_1}$$

$$2(\overline{p_4} - \overline{p_1}) \cdot \overline{p} = \overline{p_4} \cdot \overline{p_4} - \overline{p_1} \cdot \overline{p_1}$$

which is

$$\begin{aligned}(\overline{p_2 - p_1}) \cdot \overline{p} &= \frac{(p_2 + p_1)}{2} \cdot (p_2 - p_1) \\(\overline{p_3 - p_1}) \cdot \overline{p} &= \frac{(p_3 + p_1)}{2} \cdot (p_3 - p_1) \\(\overline{p_4 - p_1}) \cdot \overline{p} &= \frac{(p_4 + p_1)}{2} \cdot (p_4 - p_1)\end{aligned}$$

Since the three vectors,  $p_j - p_1$  for  $j = 2, 3, 4$ , are the edges of the tetrahedron they are linearly independent. Hence the associate matrix, namely

$$\begin{bmatrix} x_2 - x_1 & y_2 - y_1 & z_2 - z_1 \\ x_3 - x_1 & y_3 - y_1 & z_3 - z_1 \\ x_4 - x_1 & y_4 - y_1 & z_4 - z_1 \end{bmatrix},$$

is nonsingular yielding a unique solution. This solution is the center of the sphere containing the points of the tetrahedron. Solving the remaining three systems, say  $S_2, S_3$  and  $S_4$ , we find a unique solution. In each case the solution must be the center of a sphere contain the vertices of the tetrahedron. Since by the previous lemma any four non-coplanar points in 3-Space are contained in a unique sphere then the four solution sets are equal.  $\square$

*Defintion 2.10.* Let  $\mathcal{V}$  be a Voronoi Diagram generated by  $m$  points in  $\mathbf{R}^3$ . A vertex of  $\mathcal{V}$  is said to have degree  $n$  if there are at most  $n$  of the  $m$  generating points needed to generate each associated region locally.

Two regions in  $\mathbf{R}^3$  are adjacent if they share a common 2-D face.

Initially it was conjectured that the sum of the steradians of any three regions is greater than  $2\pi$ .

What is even more difficult is the claim that those regions associated with the generating points contained in the boundary of convex hull of  $X$  is infinite is not as readily seen since the process of defining the convex hull in  $\mathbf{R}^3$  is quite difficult. But we will claim the following conjecture.

*Conjecture 2.2.* Let  $X = \{X_1, \dots, X_n\}$  be a finite set of points in  $\mathbf{R}^3$ , then each Voronoi region associated with a point  $X_k$ , an element of the convex hull of  $X$  is unbounded.

This conjecture is true but the proof is omitted.

#### Voronoi Diagrams in $\mathbf{R}^2$ using the $L_\infty$ Norm.

In all of the previous work we have made use of the  $L_2$  Norm – the standard distance as defined in Euclidean space. It is based on Pythagoras' Theorem related to his theorem relating the length of the legs to the hypotenuse of a right triangle. The purpose of this section is to show that the previous results are norm dependent. Hence, for simplicity the  $L_\infty$  has been selected and all the results are done in  $\mathbf{R}^2$ .

*Definition 2.11.* For any point  $x$  in  $\mathbf{R}^2$  the  $L_\infty$  norm is given by

$$\|x\|_\infty = \max \{|x_1|, |x_2|\}.$$

To show why type of norm is significant it suffices to provide a counterexample to one of the major theorems concerning Voronoi Diagrams using the  $L_2$  Norm, namely that every nearpoint region is convex.



Example 1. Let  $x_1 = (-2, 0)$  and  $x_2 = (2, 0)$ . Figure 2.11 is the nearpoint region for  $x_1$ . Note that any shaded area defines the nearpoint region for the point  $(-2, 0)$ . Further, any point in the darker regions has as its nearpoint both  $x_1$  and  $x_2$ .

This is seen in the following argument: Since for any point in the unbounded, darker region containing  $P$  the second coordinate is larger than the first with respect to either points  $x_1$  and  $x_2$ . Hence  $\|P - x_1\|_\infty = \|P - x_2\|_\infty$  since both equal the ordinate of  $P$  because the two generating points are on the x-axis. Further, we should indicate that the Voronoi Diagram of two regions, one associated with point  $x_1$  the other with  $x_2$  result in region having infinite measure.

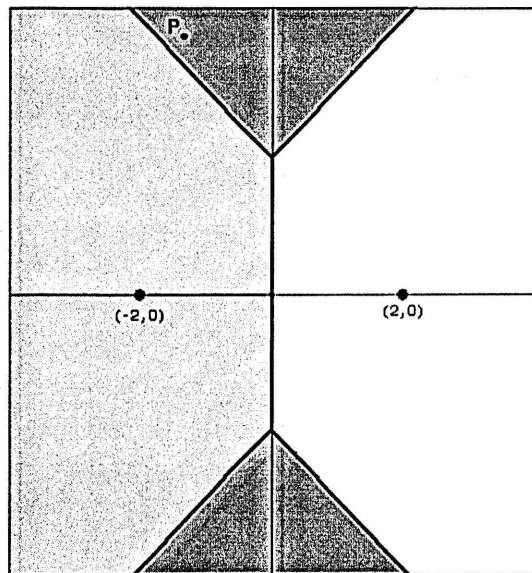


*Figure 2.11.* The shaded area, both light and dark, is the nearpoint area for  $(-2, 0)$ . Clearly it is nonconvex. Further the dark area has both generating points as nearpoints.

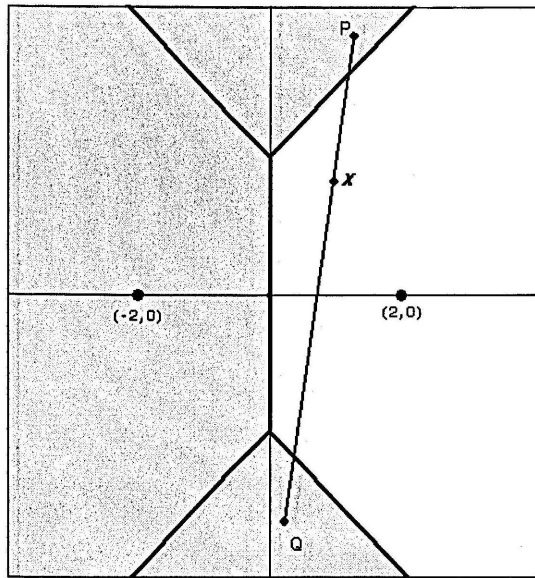


Figure 2.12. Note that the point  $X$  is not in the shaded area.

Should the points not lie on a horizontal or vertical line then the Voronoi Diagram will take the form indicated in Figure 2.13.

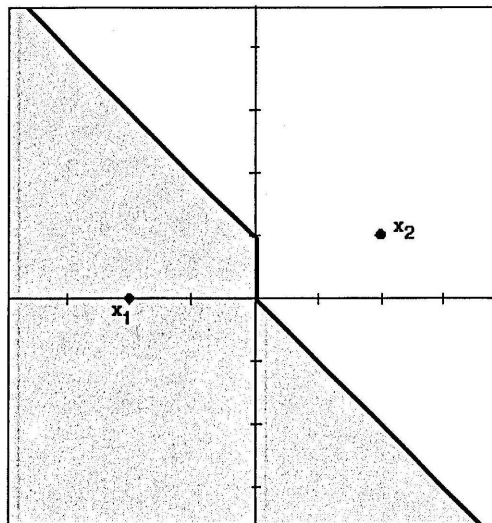


Figure 2.13. Convexity is not present for either point. The dark area and its boundary are the nearpoints associated with  $x_1$ , and the white area and its boundary are the nearpoints associated with  $x_2$ .

In closing we conjecture: If two generating points lie on a line having slope  $+1$  or  $-1$  the resulting region will be convex with the boundary being the line that is the perpendicular bisector of the line segment joining the two points.

## CHAPTER III

### INVERSE VORONOI DIAGRAM PROBLEM

#### Ray Based Characteristics of Voronoi Diagrams in $\mathbf{R}^2$ .

The concepts in this chapter resulted from the following problem: In the previous chapter we were given  $n$  points in  $\mathbf{R}^2$  which were used to generate a Voronoi Diagram. The idea here is to solve the inverse problem, that is, given a Voronoi Diagram find the generating points. Initially the problem was stated in the following question: Given a diagram that appeared to be a Voronoi Diagram can one find a set of generating points? But if we are to find the set of generating points by using the perpendicular bisector algorithm then the diagram must in fact be a Voronoi Diagram. Hence the problem required that we must somehow characterize Voronoi Diagrams since we can consider only those diagrams involving Voronoi Diagrams. If the diagram that 'looks' like a Voronoi Diagram but is in fact not a Voronoi Diagram then there would not exist a Voronoi type generating set, i.e, a set of points that will generate a Voronoi Diagram identical to the given diagram. Thus our problem is defined by the two following problems: 1. How can Voronoi Diagrams be characterized? 2. Suppose we are given a Voronoi Diagram but we are not given its generators is there an algorithm that allows us to determine the generators?

In addition we will also address the question of uniqueness with regards to the set of generating points of a Voronoi Diagram. Thus can we characterize the type of Voronoi Diagrams that have a unique generating set?

Consider the two diagrams given in Figure 3.1. The left diagram is a Voronoi Diagram since a set of three points was selected to generate the rays used to partition the plane. Diagram B was generated by drawing three rays such that the sum of two angles associated with the regions  $R_2$  and  $R_3$  sums to less than  $\pi$ .

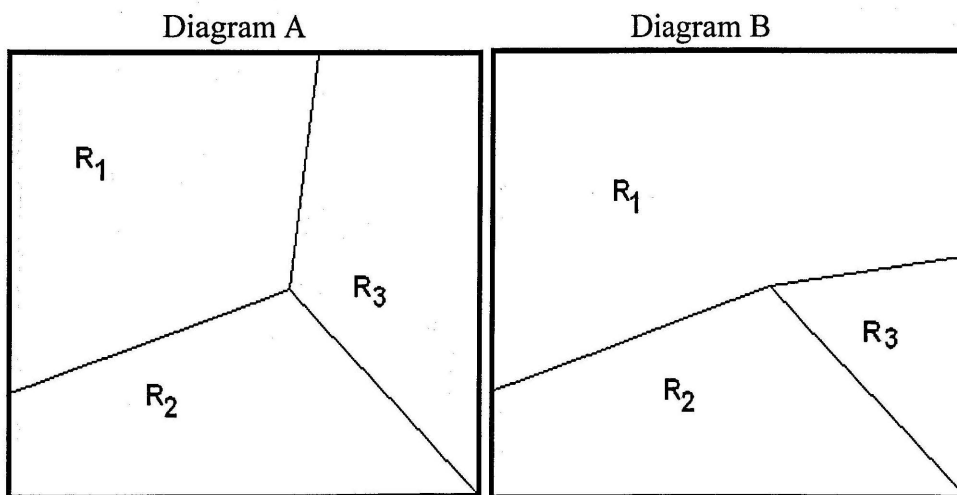


*Figure 3.1.* Diagram A is a 3-region Voronoi Diagram and Diagram B is a partition of the plane that is not a Voronoi Diagram for any three non-collinear points in the plane.

Let's begin with the question: For a given Voronoi Diagram is the set of generating points unique? The answer to this question is no as seen by the following example:

Example: Given  $\{(-2,0), (2,0), (0,2)\}$  the Voronoi Diagram is defined by the following rays:

$$\{(x, y) : (x, y) = (0, 0.1851) + \alpha(-1, 0.8149)\}_{\{(-2,0)(0,2)\}},$$

$$\{(x, y) : (x, y) = (0, 0.1851) + \alpha(1, 0.8149)\}_{\{(2,0)(0,2)\}},$$

and

$$\{(x, y) : (x, y) = (0, 0.1851) + \alpha(0, -1)\}_{\{(-2,0)(2,0)\}}$$

where  $\alpha > 0$ .

Now consider the set  $\{(-3,0),(3,0),(0,3)\}$ . For this set of points the Voronoi Diagram is defined by the same set of rays. In fact there is an infinite number of generating sets. The Voronoi Diagram for this example is given in the Figure 3.2.

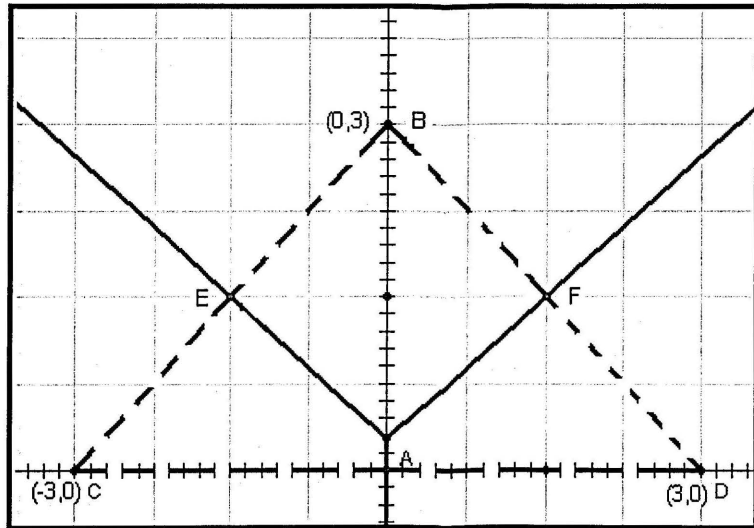


Figure 3.2. Three point Voronoi Diagram [solid] generated by the set  $\{(-3,0),(3,0),(0,3)\}$ .

Thus we have two sets of generating points for the same Voronoi Diagram.

Hence, does every Voronoi Diagram have an infinite number of generating points?

The answer to this question is found by noting that the set

$$\{(-\alpha, 0), (\alpha, 0), (0, \alpha) : \alpha \in R^+\},$$

where  $R^+$  is the set of positive real numbers, will in fact generate the same Voronoi Diagram given in Figure 3.2.

Not all Voronoi Diagrams have infinitely many generating point sets as illustrated by the following example.

Example. Given  $\{(-1, 0), (1, 0), (0, 3), (-\frac{1}{2}, \frac{1}{2})\}$  the Voronoi Diagram is defined by the following rays:

$$I1 : \{(x, y) : (x, y) = (0, -0.52) + \alpha(0, -1)\}_{\{(-1, 0)(1, 0)\}},$$

$$I2 : \{(x, y) : (x, y) = (0.69, 1.56) + \alpha(2.31, 0.77)\}_{\{(0, 3)(1, 0)\}},$$

$$I3 : \{(x, y) : (x, y) = (-2.69, 2.23) + \alpha(-1.31, 0.44)\}_{\{(0, 3)(-1, 0)\}}$$

where  $\alpha > 0$ , and the three line segments:

$$I1, I2 : \{(x, y) : (x, y) = \beta(0.00, -0.52) + (1 - \beta)(0.69, 1.56)\},$$

$$I2, I3 : \{(x, y) : (x, y) = \beta(0.69, 1.56) + (1 - \beta)(-2.69, 2.23)\},$$

$$I3, I1 : \{(x, y) : (x, y) = \beta(-2.69, 2.23) + (1 - \beta)(0, -0.52)\},$$

where  $\beta > 0$ . Also  $I1 = (0, -0.52)$ ,  $I2 = (0.69, 1.56)$ , and  $I3 = (-2.69, 2.23)$ .

The reason for the uniqueness follows from the property that the intersection of the three lines perpendicular to the resulting triangle, which is one of the generating points, is unique.

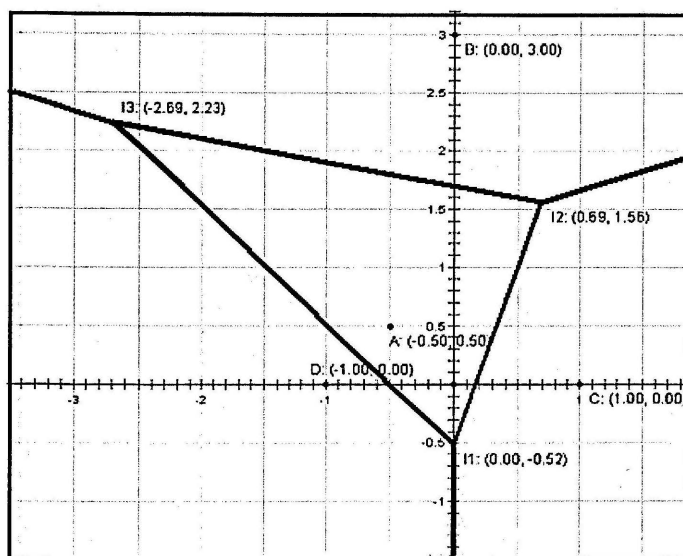


Figure 3.3. The Voronoi Diagram for the above four point case example has a unique generating point associated with the finite region.

It will be seen that a Voronoi Diagram will either have an infinite number of generating sets or there is only one unique set. Further, if the number of generating sets is infinite then the measure of all possible points is either zero or infinity. Hence, we can state the following: There is a unique generating set if and only if the Voronoi Diagram contains more than one vertex.

In addition, we note that it is well known that if there is only one vertex of a Voronoi Diagram for three or more non-collinear points then they must lie on a



circle. If the generating set has four or more points, non-cocircular<sup>7</sup> then the generating set is unique since non-cocircularity implies that the Voronoi Diagram contains at least two vertices.

*Theorem 3.1.* If a Voronoi diagram has at most one vertex then there exists an infinite number of generator sets.

*Proof. Case 1.* There are no vertices. Let  $G = \{X_1, \dots, X_n\}$  be a generating set for the diagram. In this case the Voronoi Diagram must be generated by a set of collinear generating points resulting in a diagram that consists of a set of parallel lines, each passing through the midpoint of the line segment joining each neighboring pair of generating points. Next, construct any arbitrary line,  $\mathcal{L}$ , perpendicular to the lines defining the diagram and not containing any point from  $G$ . Now construct a set of lines  $\mathcal{L}_1, \mathcal{L}_2, \mathcal{L}_3, \dots, \mathcal{L}_n$  perpendicular to the  $\mathcal{L}$  such that each  $\mathcal{L}_i$  passes through a generator point  $X_i$ . Now let  $X'_i$  denote the intersecting point of  $\mathcal{L}_i$  and  $\mathcal{L}$ . This set of points  $G' = \{X'_1, \dots, X'_n\}$  is a generating set of the Voronoi Diagram since the lines of the diagram are perpendicular bisectors of neighboring points in  $G'$ .

*Case 2.* There is one vertex. Let  $G = \{X_1, \dots, X_n\}$  be a generating set for the diagram. We recall that for any generator set of a single vertex Voronoi Diagram every elements in the generator set must be co-circular, that is, all will lie on the

---

<sup>7</sup> A set of  $n$  points in the plane is said to be non-cocircular if and only if they are not contained in a common circle.

same circle having the vertex as its center. Let  $C_G$  denote the circle containing  $G$ . Now draw a ray from the vertex  $V$  through each generator point  $X_i$ . Next pick a point,  $X'_i$ , on one of the rays distinct from the generator point. Construct a circle,  $C_{G'}$ , through the selected point with its center at  $V$ . Each remaining ray intersects the circle  $C_{G'}$  thereby defining a set of points  $G'$ , namely,  $\{X'_1, \dots, X'_n\}$ . The set  $G'$  is a generator set since for each neighboring pair  $\{X'_i, X'_{i+1}\}$  of points in  $G'$  the ray defining the diagram is the perpendicular bisector of the line segment defined by  $\{X'_i, X'_{i+1}\}$ .  $\square$

Figure 3.4 illustrate the one vertex situation given in the above argument.

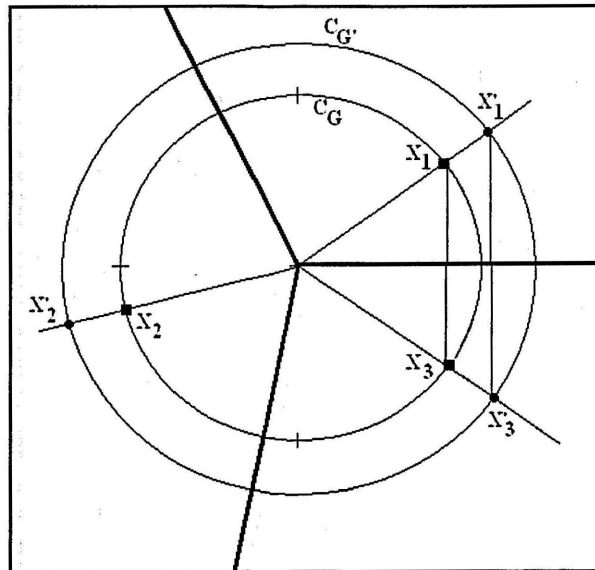


*Figure 3.4.* A geometric illustration of the argument given in the proof of Theorem 3.1.

*Theorem 3.2.* If a Voronoi diagram has two or more vertices then the generator set is unique.

Note: The following proof of Theorem 3.2 will be restricted to a Voronoi diagram with two vertices of degree 3.

Proof: Let  $V_1$  and  $V_2$  be adjacent vertices of the Voronoi Diagram,  $\mathcal{V}^o$  of order four. Let  $\mathcal{V}_1^o$  be the embedded Voronoi Diagram attached to  $V_1$  and  $\mathcal{V}_2^o$  be the Voronoi Diagram attached to  $V_2$ . Since  $V_1$  is the vertex of  $\mathcal{V}_1^o$ , a Voronoi Diagram of order one with a vertex of degree three, and  $V_2$  is the vertex of  $\mathcal{V}_2^o$  a similar Voronoi Diagram we can find two respective generator sets.

Since  $V_1$  and  $V_2$  are adjacent vertices in  $\mathcal{V}^o$ , then the joining line segment,  $\overline{V_1V_2}$ , lies on the ray  $\mathcal{R}_1$  in  $\mathcal{V}_1^o$  where  $\mathcal{R}_1 = \overrightarrow{V_1V_2}$  and concurrently lies on the ray  $\mathcal{R}_2$  in  $\mathcal{V}_2^o$  where  $\mathcal{R}_2 = \overrightarrow{V_2V_1}$ . Thus  $\overline{V_1V_2} = \overrightarrow{V_1V_2} \cap \overrightarrow{V_2V_1}$ . Now the join of  $\mathcal{V}_1^o$  and  $\mathcal{V}_2^o$  is the given Voronoi Diagram.

Now if  $G_1$  denotes a generator set of  $\mathcal{V}_1^o$  and  $G_2$  is a generator set of  $\mathcal{V}_2^o$ , then  $G_1 \cup G_2$  is not a generator set of  $\mathcal{V}^o$  unless  $\#(G_1 \cap G_2) = 2$  where  $\#(G_1 \cap G_2)$  denotes the cardinality of the set  $G_1 \cap G_2$ . Generally  $\#(G_1 \cap G_2)$  is not equal to two, hence we select  $g_1 \in G_1$  such that the interior of the region containing  $g_1$ , say  $R_{G_1}$ , intersects the interior of a region of  $G_2$ , say  $R_{G_2}$ . Let  $L(V_1, g_1)$  containing  $V_1$

and  $g_1$ . Now there exist a point  $g_2$  in the generator set  $G_2$  such that  $g_2 \in R_{G_2}$ . Let  $L(V_2, g_2)$  denote the line through  $V_2$  and  $g_2$ . The lines  $L(V_1, g_1)$  and  $L(V_2, g_2)$  are not parallel hence they intersect at a point  $g^*$  in the region  $R_{G_1} \cap R_{G_2}$ . Since  $g^*$  is on the lines  $L(V_1, g_1)$  and  $L(V_2, g_2)$  then  $g^*$  is an element of a generator set for  $\mathcal{V}_1$  and  $\mathcal{V}_2$ . Using this point we reflect it through each ray in  $\mathcal{V}_1$  and each ray in  $\mathcal{V}_2$  generating the sets  $G_1^*$  and  $G_2^*$  such that each is a generator set of  $\mathcal{V}_1$  and  $\mathcal{V}_2$  respectively and  $\#(G_1^* \cup G_2^*) = 4$ . Hence  $G_1^* \cup G_2^*$  is a generator set of the original Voronoi Diagram  $\mathcal{V}$ . Since the intersection of the two lines is unique the set  $G_1^* \cup G_2^*$  is unique.  $\square$

The following figures are an illustration of the proof.

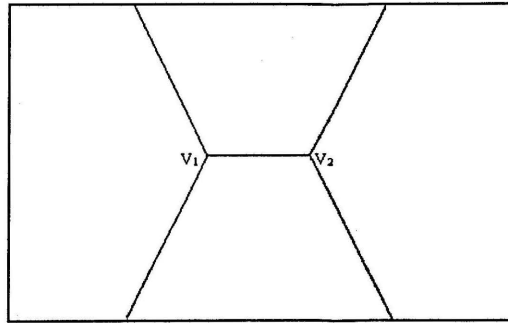


Figure 3.5. The original Voronoi Diagram.

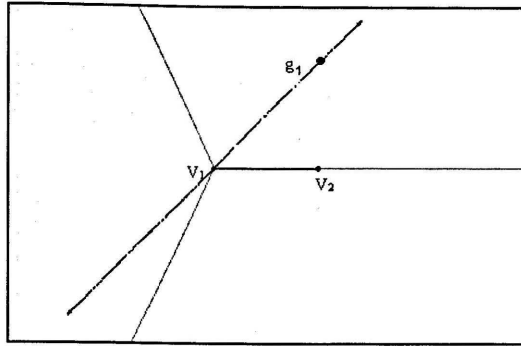


Figure 3.6. Using  $V_1$  we define the Voronoi Diagram  $\mathcal{V}_1$ .

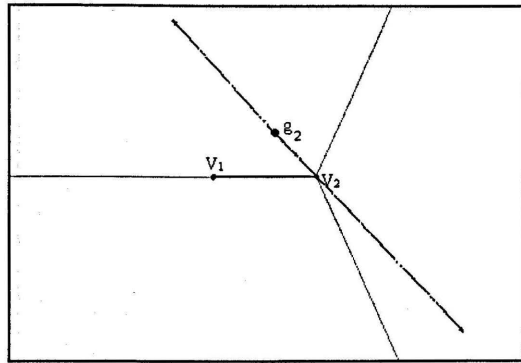


Figure 3.7. Using  $V_2$  we define the Voronoi Diagram  $\mathcal{V}_2$ .

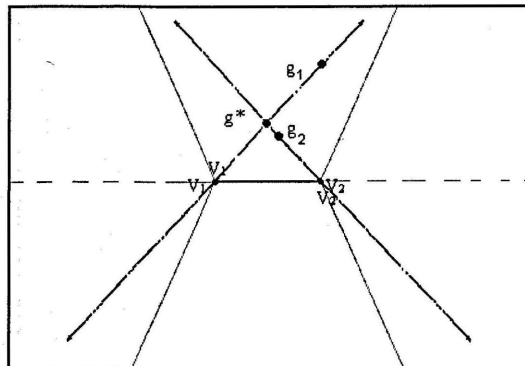


Figure 3.8. Aligning the two Voronoi Diagrams  $\mathcal{V}_1$  and  $\mathcal{V}_2$  we have the resulting diagram with the two intersecting lines.

The converse of Theorems 3.1 and 3.2 is given in the following conjectures.

*Conjecture 3.1.* (Zimmermann) If a Voronoi diagram has an infinite number of generator sets then the Voronoi Diagram has at most one vertex.

*Conjecture 3.2.* (Zimmermann) If a Voronoi diagram has a unique generator set then the Voronoi Diagram has at least two vertices.

### Inverse Voronoi Diagrams in $\mathbb{R}^2$ .

We now consider the problem: Given the Voronoi Diagram but not given the generating points how can we find the generating points?

In this section we will develop a numerical algorithm for determining the generating set(s) of a Voronoi Diagram. We will address this problem with regard to the number of vertices contained in the diagram. Hence we will begin with those diagrams having no vertices, followed by those having one vertex and finally those having two vertices. The situation in which the diagram has more than two vertices is beyond the scope of this thesis.

#### *Case 1. Zero Vertices.*

No vertices implies that the Voronoi Diagram consists of parallel lines and results from the colinearity of the generator points,  $\mathcal{G}$ . Since the rotation and translation of such a Voronoi Diagram results in a isometric, topologically equivalent diagram we will assume that the generators lie on the x-axis. Hence we let  $\mathcal{V}_0$  equal the class of Voronoi Diagrams having no vertices and perpendicular to the x-axis.

Next we note that there are infinitely many generator sets for any Voronoi Diagram in the class of Voronoi Diagrams having no vertices. This is seen in the following argument: If  $G = \{(x_i, 0) : x_i \in R^1, i = 1, \dots, n\}$  is a generator set of a particular Voronoi Diagram in this class, then  $G$

$= \{(x_i, y) : x_i \in R^1, i = 1, \dots, n, y \in R^1\}$  is also a generator set.

We are now positioned to address the inverse problem as it relates to the class,  $\mathcal{V}_0$ , of Voronoi Diagrams. Suppose we are given a Voronoi Diagram in  $\mathcal{V}_0$  but not its generator set, determine a generator set.

Since the lines are pairwise parallel and all are perpendicular to the x-axis this problem can be stated as follows: Given a set of points on the x-axis, intersections of the Voronoi Diagram with the x-axis. Find a set of points

$$G_R = \{x_i : x_i \in R, i = 1, \dots, n\}$$

such that  $G = \{(x_i, 0) : x_i \in R^1, i = 1, \dots, n\}$  is a generator set of the associated Voronoi Diagram.

We first order the points in  $G$ . Next we let  $x_i^g$  denote the unknown point of  $G$  that lies between each adjacent point  $x_i$  and  $x_{i+1}$ . Further  $x_0^g$  and  $x_n^g$  represents the points in such that  $x_0^g$  is less than all values in  $G$  while  $x_n^g$  is greater than all values in  $G$ . From this geometry we have

$$\|x_0^g - x_1\| = \|x_1^g - x_1\|$$

$$\|x_1^g - x_2\| = \|x_2^g - x_2\|$$

$$\|x_2^g - x_3\| = \|x_3^g - x_3\|$$

$$\|x_3^g - x_4\| = \|x_4^g - x_4\|$$

This system can then be written as

$$x_0^g x_0^g - 2x_0^g x_1 + x_1 x_1 = x_1^g x_1^g - 2x_1^g x_1 + x_1 x_1$$

$$x_1^g x_1^g - 2x_1^g x_2 + x_2 x_2 = x_2^g x_2^g - 2x_2^g x_2 + x_2 x_2$$

$$x_2^g x_2^g - 2x_2^g x_3 + x_3 x_3 = x_3^g x_3^g - 2x_3^g x_3 + x_3 x_3$$

$$x_3^g x_3^g - 2x_3^g x_4 + x_4 x_4 = x_4^g x_4^g - 2x_4^g x_4 + x_4 x_4$$

Simplification yields

$$2(x_1^g - x_0^g)x_1 = x_1^g x_1^g - x_0^g x_0^g$$

$$2(x_2^g - x_1^g)x_2 = x_2^g x_2^g - x_1^g x_1^g$$

$$2(x_3^g - x_2^g)x_3 = x_3^g x_3^g - x_2^g x_2^g$$

$$2(x_4^g - x_3^g)x_4 = x_4^g x_4^g - x_3^g x_3^g$$

which gives the system

$$\begin{bmatrix} 1 & 1 & 0 & 0 & 0 \\ 0 & 1 & 1 & 0 & 0 \\ 0 & 0 & 1 & 1 & 0 \\ 0 & 0 & 0 & 1 & 1 \end{bmatrix} \begin{bmatrix} x_0^g \\ x_1^g \\ \vdots \\ x_4^g \end{bmatrix} = \begin{bmatrix} 2x_1 \\ 2x_2 \\ 2x_3 \\ 2x_4 \end{bmatrix}$$

Since the matrix has rank four with five unknowns we write

$$\begin{bmatrix} 1 & 1 & 0 & 0 \\ 0 & 1 & 1 & 0 \\ 0 & 0 & 1 & 1 \\ 0 & 0 & 0 & 1 \end{bmatrix} \begin{bmatrix} x_0^g \\ x_1^g \\ x_2^g \\ x_3^g \end{bmatrix} = \begin{bmatrix} 2x_1 \\ 2x_2 \\ 2x_3 \\ 2x_4 - x_4^g \end{bmatrix}$$

The inverse of



$$\begin{bmatrix} 1 & 1 & 0 & 0 \\ 0 & 1 & 1 & 0 \\ 0 & 0 & 1 & 1 \\ 0 & 0 & 0 & 1 \end{bmatrix}$$

is

$$\begin{bmatrix} 1 & -1 & 1 & -1 \\ 0 & 1 & -1 & 1 \\ 0 & 0 & 1 & -1 \\ 0 & 0 & 0 & 1 \end{bmatrix}.$$

Hence a solution is

$$\begin{bmatrix} x_0^g \\ x_1^g \\ x_2^g \\ x_3^g \end{bmatrix} = \begin{bmatrix} 1 & -1 & 1 & -1 \\ 0 & 1 & -1 & 1 \\ 0 & 0 & 1 & -1 \\ 0 & 0 & 0 & 1 \end{bmatrix} \begin{bmatrix} 2x_1 \\ 2x_2 \\ 2x_3 \\ 2x_4 - x_4^g \end{bmatrix}$$

Hence

$$x_0^g = 2(x_1 - x_2 + x_3 - x_4) + x_4^g$$

$$x_1^g = 2(x_2 - x_3 + x_4) - x_4^g$$

$$x_2^g = 2(x_3 - x_4) + x_4^g$$

$$x_3^g = 2x_4 - x_4^g$$

### *Case 2. One Vertex.*

In this situation we will begin by assuming that the vertex is of degree three.

Next we translate the Voronoi Diagram so that the vertex lies on the origin. We

then rotate the diagram so that one of the rays is concurrent with the positive x-axis.

We now construct a circle of arbitrary radius with the origin, the vertex, as its center. Let  $\theta_1$  denote the angle between the intersection of the circle with the x-axis and the intersecting point of the first ray encountered moving in the counterclockwise direction. Thus  $\theta_1 = \angle \beta_1 V \beta_2$ . Select the initial guess  $X_1$  at such that the angle is  $\theta_1/2$ . Generate by reflection through each ray the points on the circle  $X_2, X_3$ , and  $X_4$ . Next, let  $X'_1$  be the midpoint between  $X_1$  and  $X_4$ . Reflect  $X'_1$  through the rays of the Voronoi Diagram generating  $X'_2, X'_3$  and  $X'_4$ . Initially it was thought that this method would yield better and better approximations. What has been found is that  $X'_4$  and  $X'_1$  are the same. Hence, the set  $\{X'_1, X'_2, X'_3\}$  is a generator set for the Voronoi Diagram.

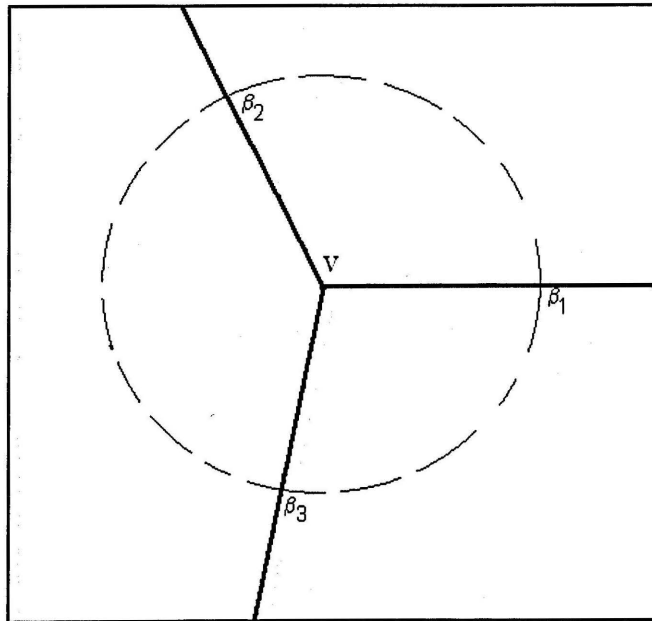


*Figure 3.9.* The initial Voronoi Diagram with the  $\beta$ 's indicating the intersection of the rays with the overlaid circle.

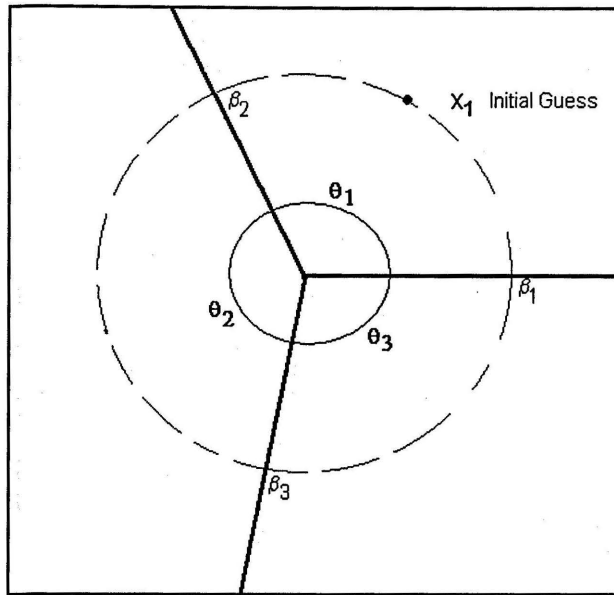


Figure 3.10. The angle of each region is represented by  $\theta_k$ ,  $k = 1, 2, 3$ ; moving in a counterclockwise direction.

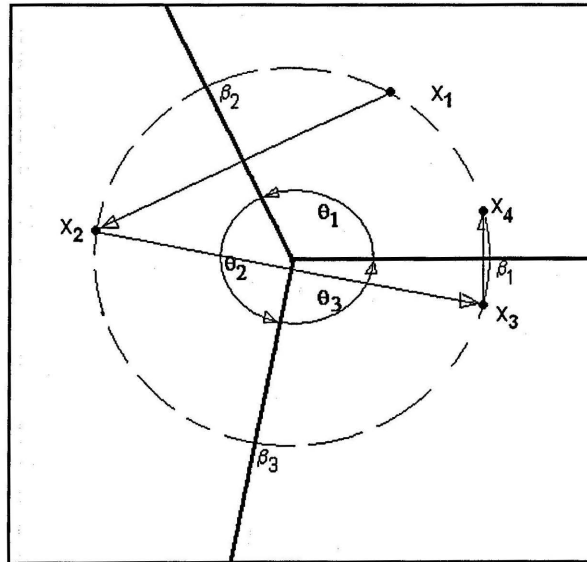


Figure 3.11. An initial guess  $X_1$  is made then reflected through each ray, generating the set  $\{X_1, X_2, X_3, X_4\}$ . Next the midpoint between  $X_1$  and  $X_4$  is used to the next generating point.

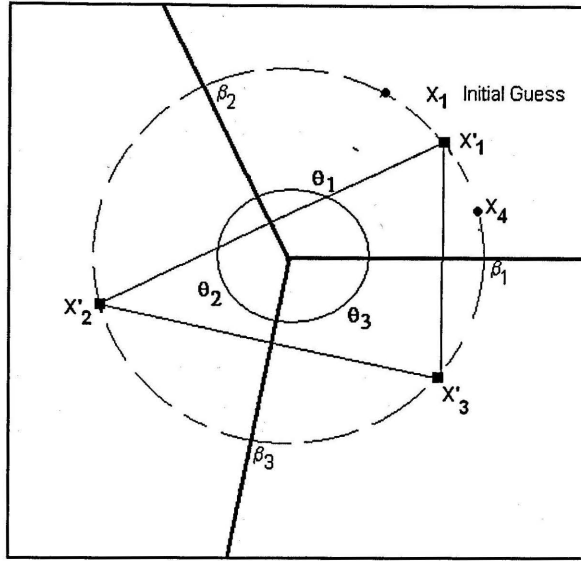


Figure 3.12. Using  $x'_1$  reflection is applied to generate the set  $\{x'_1, x'_2, x'_3\}$  which is a generator set for the Voronoi Diagram.

Note, the circle was arbitrary and hence we have that since any circle can be used to determine a generator set for the Voronoi Diagram there is an infinite number of solutions. We have not proved that the result midpoint is the generator of the generating set because it was found that a shorter method could be had. Initially, the angel  $\eta$  formed by the x-axis and the ray through the 'first' generating point could be found by noting that

$$\begin{aligned}
 &\eta \\
 &\theta_1 - \eta \\
 &\theta_2 - (\theta_1 - \eta) \\
 &\theta_3 - (\theta_2 - (\theta_1 - \eta)) = \eta \\
 \Rightarrow &\eta = \frac{\theta_1 - \theta_2 + \theta_3}{2}
 \end{aligned}$$

which can be seen in the following figure and the fact that fourth equation in the above is required if the set is to be a generator set.

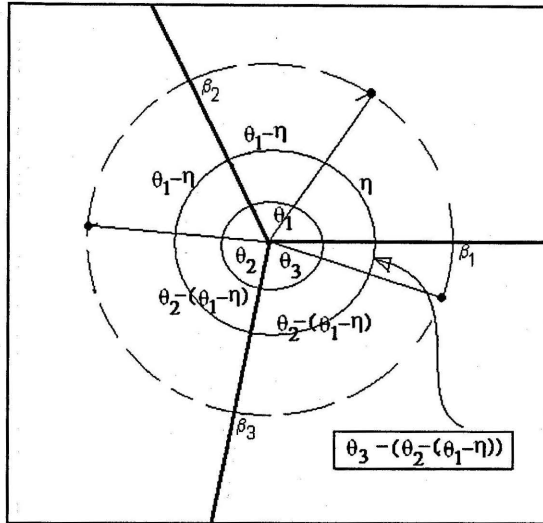


Figure 3.13. The relationship between the angles as they are reflected through each ray.

We have discussed the problem for a Voronoi Diagram having a single vertex of degree 3. But what if the vertex is of degree  $n$ ,  $n$  greater than three? What has been found is given in the following conjectures.

*Conjecture 3.3.* (Zimmermann) Given a Voronoi Diagram with one vertex of degree  $n$  where  $n$  is even then  $\sum_{k=1}^n (-1)^{k+1} \theta_k = 0$  where each  $\theta_k$  is measured in a counterclockwise direction and each region is indexed in an increasing sequence as we move counterclockwise.

This conjecture implies that one can pick any point in the 'first' region. Draw a circle through that point having center  $V$  then reflect the point and its resulting points through each and every ray of the Voronoi Diagram giving a generating set.

*Conjecture 3.4.* (Zimmermann) Given a Voronoi Diagram with one vertex of degree  $n$  where  $n$  is odd then  $\eta = \frac{1}{2} \sum_{k=1}^n (-1)^{k+1} \theta_k$  where the thetas are measured in a counterclockwise direction. Then any point on the ray making an angle  $\eta$  can be used as the initiator of the generator set of the given Voronoi Diagram.

From these two conjectures we can conclude that depending on the structure of the Voronoi Diagram the regions defined by the generator sets is either a finite set, or an unbounded set of measure zero or an unbounded set of measure infinity. The proof of the conjectures will not be given in this thesis.

*Case 3. Two Vertices.*

This case can be reduced to the previous case by use of the technique given in Theorem 3.2.

*Case 4. Three or more Vertices.*

This case can be reduced to Case 3 by selecting two adjacent vertices of degree 3 then surgically removing the embedded Voronoi Diagram defined by the selected vertices. Once a generator point is obtained for the selected Voronoi Diagram we can then determine the generating set, which will be unique.

## CHAPTER IV

### CONCLUSION AND OPEN PROBLEMS

#### Conclusions

In closing it should be noted that our primary results are directed towards the development of a solution for the inverse problem. The idea being based on a number of applications which are generally posed as: given the several locations what is the set of points having the given location as their nearpoint? Related problems include: Fire Observation Towers – Imagine a large forest containing a number of ranger stations supplied with fire fighting equipment. Suppose a fire occurs at some point. There is the problem of finding the nearest station. Further, one could ask a related question: what region of the forest has a particular station as its nearpoint. It is this question that defines the Voronoi Diagrams.

Given this problem we wanted to solve the following problem: if a forest is partitioned into  $n$  regions, with the property that in each region a station will be built, where should it be located if the resulting locations of all stations are to yield a Voronoi Diagram equivalent to the given partitioning? And can any partition be made equivalent to some Voronoi Diagram? Our conclusion is: No. The proof of nonequivalence is immediate if the given partition includes a region that is not convex. Hence, we decided to address a simpler problem: Given a Voronoi Diagram, but not the generating points, how can we determine the generating points? Coupled to this question is the question

of uniqueness. With regards to this property we found that non-uniqueness occurred if and only if the Voronoi Diagram has at most one vertex, that is, the generating set is contained in a single circle.

Other application of Voronoi Diagrams include: the study of crystallography and biology. In the problem of crystallography assume a number of crystal seeds grow at a uniform rate. What will be the appearance of the crystal when growth is no longer possible? Similarly, this question can be asked with regards to biological growth. What if the rate is not uniform?

### Open Problems

An immediate extension might be had by extending the concept of Voronoi Diagram to the surface of a sphere,  $S^2$  or  $S^n$ . In the case of  $S^2$  for any two points in the boundary of the two regions defining the set of points having one of the given points as its nearpoint is the great circle that is perpendicular to the short arc contained in the great circle containing the two given points. How would the surface be partitioned for three points? How would it be partitioned for  $n$  points? Is every region convex?

In the crystallography problem one could address the following: what will the crystal look like if the rates vary among the crystal seeds? Actually, the answer to this question would assist in modeling a number of biological growth problems. Further, it



appears that the Voronoi Diagram can be obtained by means of a Diffusion Equation<sup>8</sup> with multiple sources and isotropic diffusion.

Lastly, we should note that Voronoi Diagrams have been studied at length with respect to finite set, but what properties would carry over if the generator set is infinite?

---

<sup>8</sup> Diffusion Equation is given by the partial differential equation:  $u_t = \alpha u_{xx}$ .

## BIBLIOGRAPHY

- Mathews, J. H., and Kurtis D. Fink, (2004), *Numerical Method Using MATLAB*, Prentice Hall, Upper Saddle River, New Jersey.
- Noyes, James & Eric Weisstein, "Linear Programming," Math World—A Wolfram Web Resource, <http://mathworld.wolfram.com/LinearProgramming.html> (accessed November 17, 2006)
- Beyer, W. A. & Zardecki, Anderw (2004). „The Early History of the Ham Sandwich Theorem“, *American Mathematical Monthly* 111(1), 58-61.
- O'Rourke, J., (1998), *Computational Geometry in C* (2nd 2<sup>nd</sup> ed.). New York, NY: Cambridge University Press.
- De Berg, M., van Kreveld, M., Overmars, M. & Schwarzkopf, O. (2000). *Computational Geometry* (2nd ed.). New York, NY: John Wiley & Sons, Inc.
- Preparata, F. P. & Shamos, M. I. (1985). *Computational Geometry: An Introduction*. New York, NY: Springer-Verlag.
- Okabe, A., Boots, B., & Sugihara, K. (1992). *Spatial Tessellations: Concepts and Applications of Voronoi Digrams*. New York, NY: John Wiley & Sons, Inc.
- Aurenhammer, F. & Klein, R. *Voronoi Diagrams*. Preprint supported by the Deutsche Foreschungsgemeinschaft, grant K1 655 2-2.